**Title**
DEVELOPMENT OF A JET-MIXED EXTRACTION COLUMN



**Authors**
Kahn, Daniel R.
Vermeulen, Theordore.

**Publication Date**
1969-02-01

UCRL-18679

# DEVELOPMENT OF A JET-MIXED EXTRACTION COLUMN

Daniel R. Kahn* and Theodore Vermeulen

February 1969

AEC Contract No. W-7405-eng-48

*M. S. Thesis



LAWRENCE RADIATION LABORATORY
UNIVERSITY of CALIFORNIA BERKELEY

UCRL-18679

## DISCLAIMER

# DEVELOPMENT OF A JET-MIXED EXTRACTION COLUMN

## Contents

# DEVELOPMENT OF A JET-MIXED EXTRACTION COLUMN

Daniel R. Kahn[b] and Theodore Vermeulen[a]

Department of Chemical Engineering and
Lawrence Radiation Laboratory
University of California
Berkeley, California

February 1969

## ABSTRACT

A jet-mixed extraction column has been developed which incorporates most advantages of existing column-type extractors, while eliminating the need for internal moving parts. The column was designed to provide high rates of mass transfer, with only normal or even decreased extents of unwanted longitudinal dispersion ("axial mixing"). A guide to some of the more important experimental studies involving longitudinal dispersion in various column-type extractors, and two theoretical models which describe the combined effect of mass transfer and longitudinal dispersion, are presented.

The concept of a jet-mixed column is discussed, and the apparatus employed in the present study is described. The column utilizes uniformly spaced, horizontal, tubular, jetting and intake rings at the inner and outer boundaries of an annular cross-section. At each level, both rings are perforated so as to promote nearly straight-line radial flow between the jetting and intake rings. Externally these rings are connected by way of a small centrifugal circulating pump.

Semiquantitative tests of the column in single-phase and two-phase operation have been made to study the effects of number, size, and position of the ring ports, compartment height, jetting circulation rate, and longitudinal flow rates, upon the vortex patterns, the extent of interception (desired) of the discontinuous phase, and the extent of colloidal dispersion (undesired) of discontinuous phase.

Further experimentation, involving a complete mass-transfer analysis using two different solvent-solute systems and a larger number of jet-mixed stages, is needed to complete the performance evaluation of this new design.

# LIST OF TABLES

# LIST OF FIGURES

Figure

# I. INTRODUCTION

## A. Types of Extractors

### 1. General Considerations

Commercial extraction equipment can be divided into two main categories, depending on whether the mode of operation is staged or column-type. Several reviews (2,10,20,41,45) of industrial extractors have been published which describe the operation, application, and attributes of the more common designs in each of these groups. The purpose of the present study is to explore the feasibility of a new design which incorporates many of the advantages of existing column-type extractors while eliminating the need for internal moving parts.

Stagewise contacting is characterized by a dispersion of one phase into a second phase, followed by a complete settling and separation of the two liquids. Each two-step cycle constitutes one stage in the extraction process. The total desired mass transfer is usually achieved by a cascade of stages with countercurrent feeding of the two phases. Although such mixer-settlers provide good contacting, are highly efficient, and can be scaled up with some degree of reliability, they also require considerable liquid holdup, large floor area, extensive piping, and relatively high power costs and initial investment.

In an attempt to combine the basic advantages of staged extractors with such attributes as high capacity, low residence time, and the ability to handle systems with wide ranges of flow ratios, engineers have developed various column-type extractors. In such equipment, both phases

are in continual contact; the dispersed phase remains in the form of uncoalesced small droplets, while the continuous phase follows a flow path that is relatively uninterrupted through the entire column. It is possible to subdivide column-type contactors into two main groups, depending on whether external power has been added to promote interphase dispersion. Those involving external power are further classified according to the force field used to transport and separate the two phases. Table 1 summarizes the various groups of column-type extractors and lists several well-known examples in each case. A description of column-type extractors involving centrifugal transport can be found in Ref. (2) and (20).

2. Column-Type Extractors---No External Power

Column-type extractors involving no form of external mechanical power utilize the density difference between the two phases in a gravitational field to produce countercurrent flow and increase interfacial area. Some operate in a differentially continuous manner, as in spray and packed towers, while others are "semi-staged", as in perforated-plate towers. The major attribute of these columns is their simplicity in design and operation. Futhermore, maintenance costs are kept low, since there are no internal moving parts. Where difficult separations are to be made involving many transfer units or stages, more sophisticated equipment is needed which provides for increased efficiency and capacity, relatively easy scale-up, and reasonable cost.

Table 1

Classification of Column-Type Extractors

I. No external power

- A. Spray column
- B. Packed column
- C. Perforated-plate column

II. External power added

- A. Gravity transport
  - 1. Pulsation
    - a. Pulsed-packed column
    - b. Pulsed sieve-plate column
  - 2. Mechanical agitation
    - a. Scheibel column
    - b. Rotating-disc column
    - c. Oldshue-Rushton column
- B. Centrifugal transport
  - 1. Podbielniak extractor (44)
  - 2. Westfalia extractor (14)

3. Column-Type Extractors---External Power Added

The efficiency of gravity-powered columns may be significantly improved by utilizing some method to introduce mechanical energy into the flowing liquids. Mechanical agitation increases the scale of turbulence, creating a higher interfacial area and minimizing the diffusional resistances in both phases. As a result, the rate of mass transfer is increased, enabling many theoretical stages to be contained in a single column. One undesirable feature which may be produced by the intense mixing is the phenomenon of backmixing in both the continuous and dispersed phases. Most designs have incorporated some form of baffling to localize and minimize this effect. A more detailed description of backmixing or "longitudinal dispersion" and its effect upon mass transfer will be presented in Section I-B.

a. Pulsed Columns

Numerous investigators have found that the efficiencies of packed-bed columns (8,9,15,40,53,65) and perforated-plate columns (13,15,56,57,61) can be improved by a factor of two or three by applying a pulsing flow to the contents of the column. Pulsation aids in breaking up the dispersed-phase droplets by intensifying the turbulence, thus creating a larger interfacial area for mass transfer. Obtaining a uniform dispersion in large diameter columns, however, may be a problem.

For plate columns, pulsing simplifies the construction. Upcomers and downcomers are no longer necessary; the plates extend over the entire cross-section of the column. In operation, the light phase under each

plate is forced through the perforations on the up stroke and dispersed into the next stage. The heavy phase is drawn down on the opposite stroke. The nuclear industry has maintained a major interest in pulsed-plate columns because of their high efficiency and lack of internal moving parts.

b. Mechanically-Agitated Columns---Gravity Transport

The Scheibel column (49,51) illustrated in Figure 1a is one of several variants of the same general principle which has been used in industrial processes. In the alternate sections of mixing and settling provided, dispersion is created by turbine-type impellers driven by a central rotating shaft, while wire-mesh packing of 95-98% void volume aids in coalescence.

The rotating-disc column (46) developed by G. H. Reman has also found wide industrial acceptance. It is highly efficient, simple to maintain and operate, and may well have the most economical construction for any specified capacity and efficiency. The rotating-disc column (RDC), unlike the Scheibel column, does not provide for any interstage coalescence. As shown schematically in Figure 1b, the RDC consists of a number of compartments formed by stator rings supported at the tower wall. Midway between each pair of rings is a flat disc mounted on a central rotating shaft. The stator opening is slightly greater than the diameter of the rotating disc, enabling the entire shaft assembly to be removed for maintenance purposes. An extra stator ring

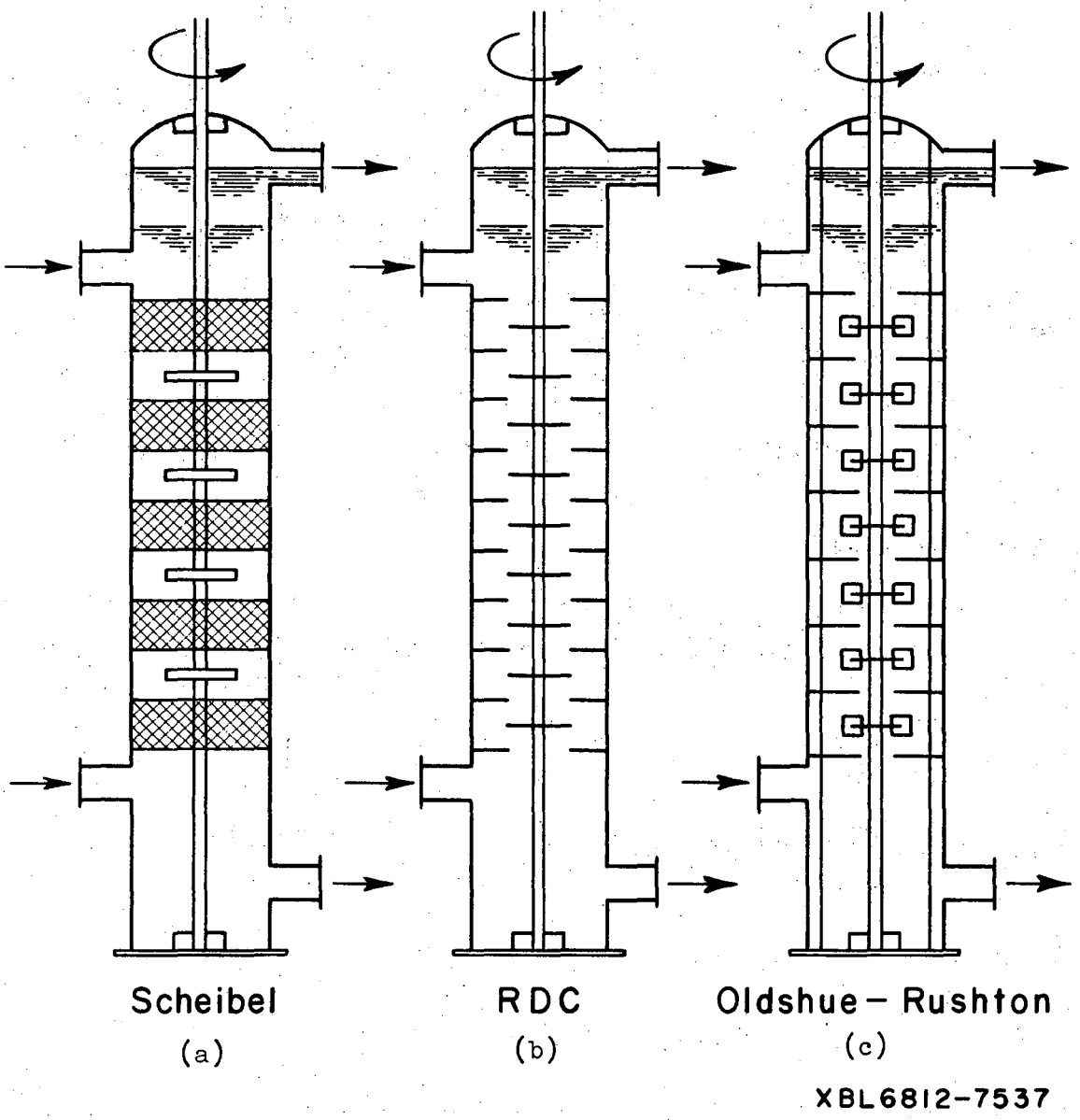


Fig. 1. Mechanically-aided column-type extractors (adapted from Ref. 1).

and a wire mesh grid are provided at each end of the column to promote coalescence and to minimize disturbances in each settling compartment.

Flow within each stage of the RDC involves two steady-state vortices of opposite sense, as illustrated in Figure 2a. Dispersion of the discontinuous phase is produced by the turbulence of the vortices due to the action of the rotating discs. The stator rings reduce interstage mixing by diverting the liquid flowing along the walls into the center of each stage.

The Oldshue-Rushton column (42) shown in Figure 1c is similar to the RDC, having a central rotating shaft, with annular rings to separate the tower into a series of mixing cells. Turbine-type blade impellers located midway between each pair of rings create the dispersion, while vertical baffles extending from the wall enhance agitation and improve efficiency. The stages of the Oldshue-Rushton column are usually deeper, and the stator openings smaller than in the RDC, resulting in additional flow compartmentalization. Settling zones are again provided at the upper and lower ends of the column. The vortex motion created within each stage of the Oldshue-Rushton column resembles that in the RDC, as illustrated in Figure 2b.

Table 2 lists some of the factors which affect the performance of both the rotating disc and Oldshue-Rushton columns. The data show how the capacity and efficiency will change for an increase in each given variable. It is evident that the final design of either type of extractor will depend upon the relative importance of high column throughput and of high column efficiency.

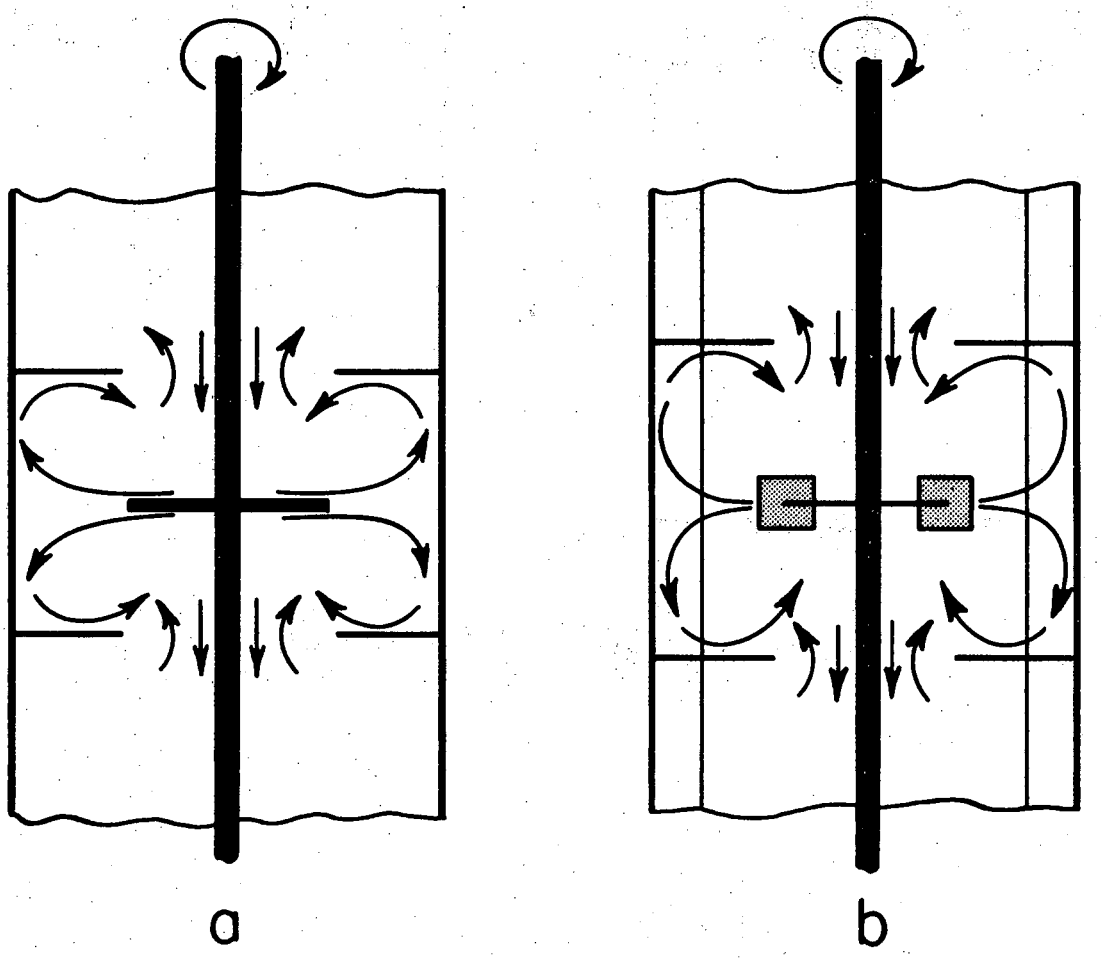


Fig. 2. Flow patterns in the (a) rotating-disc and (b) Oldshue-Rushton columns.

Table 2

Variables Affecting the Performance of Both Rotating-Disc and Oldshue-Rushton Columns

| Increasing Variable | Capacity ($lbs/hr \cdot ft^2$) | Efficiency ($\frac{\text{theor. stages}}{\text{ft. column ht.}}$) |
|---|---|---|
| Agitator speed, N (rev/hr) | decreases | increases* |
| Agitator diameter, R (ft) | decreases | increases |
| Diameter of stator opening, $d_s$ (ft) | increases | decreases |
| Compartment height, $h_c$ (ft) | increases | decreases |
| Tower diameter, D (ft) | constant** | constant** |
| Phase ratio, $V_d/V_c$ ($\frac{ft/hr}{ft/hr}$) | increases | increases |

*May pass through a maximum owing to backmixing at high N.

**At constant R/D.

## B. Longitudinal Dispersion in Solvent-Extraction Columns

### 1. The Phenomenon of Longitudinal Dispersion

It is recognized widely that longitudinal dispersion, or axial mixing, may substantially reduce the performance of continuous countercurrent solvent-extraction columns. Longitudinal dispersion is particularly evident in mechanically aided contactors, where fluid-flow aspects can limit column operation even though interphase dispersion and mass-transfer rates are high. The goal of rational design of extraction equipment therefore produces an incentive for a thorough understanding of the mechanism and effects of longitudinal dispersion.

Longitudinal dispersion is the result of several effects:

(1) Continuous-phase "backmixing", due to

- true turbulent and molecular diffusion along the axis of the extractor;
- local eddy motion and entrainment of fluid in the wakes of rising dispersed phase droplets;
- radial diffusion owing to a nonuniform velocity profile across the column.

(2) Dispersed-phase "backmixing" caused by

- local high velocities of continuous phase eddies;
- a distribution of residence times for the dispersed phase owing to the initial drop size distribution.

(3) Channeling flow due to the particular column internals.

The above mechanisms, whether acting separately or in combination, reduce the concentration driving force for mass transfer; thereby a longer column (for any given mass-transfer coefficient) is required to achieve the same overall separation. Figure 3 shows schematic concentration profiles in a liquid-liquid extractor, where

Z = dimensionless length variable, ranging from zero at the X-feed end to unity at the Y-feed end of the column,

$c_i$ = concentration of solute in phase i, gram-moles/cc. The number accompanying c, if a subscript, is the Z value inside the column; if it is a superscript (0 or 1), it is the Z value in the feed or product stream outside the column, and

m = slope of equilibrium curve, $dc_x^*/dc_y$.

The broken lines (AD'E and FH'K) represent true countercurrent flow; the solid lines (ABDE and FGHK), accounting for the effect of longitudinal dispersion, exhibit a sharp jump in concentration as each phase enters the column. The decrease in driving force is shown by the vertical arrows.

During the past fifteen years, the phenomenon of longitudinal dispersion in solvent extraction columns has been studied by many investigators. The subject has recently been reviewed by Vermeulen and co-workers (63), Li and Ziegler (30), and Hanson (21). Research effort in the field can be divided into two major areas: the study of the

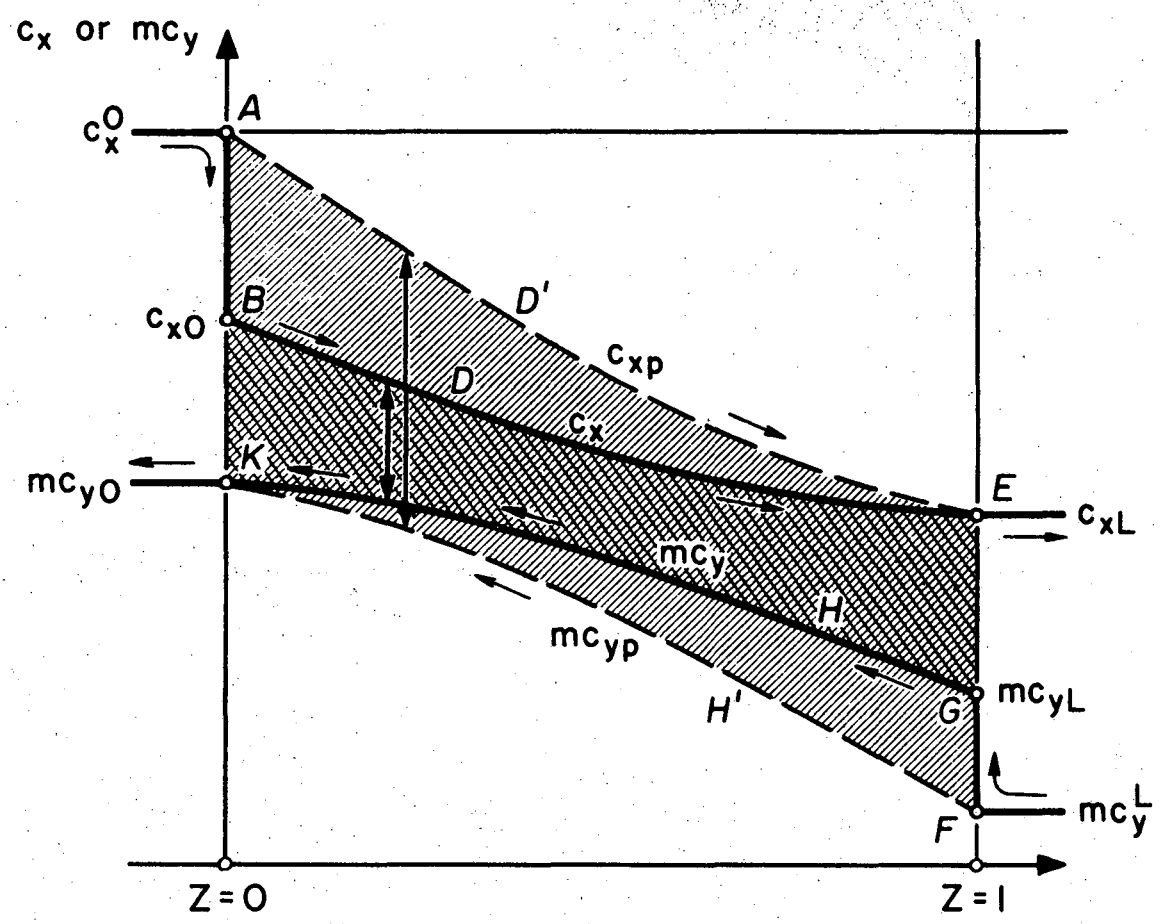


MU-14083

Fig. 3. Schematic concentration profiles in a typical extraction.

degree of backmixing in various column-type extractors, and the development of mathematical models which describe the combined effect of mass transfer and longitudinal dispersion. The models have been particularly useful in interpreting and correlating experimental data for the design of new extractors. A guide to some of the more important experimental studies is presented in Table 3.

2. Theoretical Models Describing Longitudinal Dispersion

a. Backflow Model

Two useful approaches have been developed to account for longitudinal dispersion in solvent-extraction columns. The first is the backflow model proposed by Miyauchi and Vermeulen (39). Shown schematically in Figure 4, the model consists of a series of well-mixed stages in cascade with a backflow of each stream superimposed upon the net flows through the column. The net volumetric flow rates between adjacent stages are denoted by $\overline{F}_x$ and $\overline{F}_y$, while a reverse flow occurring in each direction, F, is given by the sum of the individual backflows for each phase, $F_x$ and $F_y$. The total interstage flows for phases X and Y are therefore $(\overline{F}_x+F_x+F_y)$ and $(\overline{F}_y+F_y+F_x)$, respectively.

To formulate the basic equations for the model, X will be designated as the continuous phase and Y the dispersed phase, with mass transfer occurring from phase X to phase Y. To simplify the analysis, it will be assumed that sufficient coalescence and redispersion of the discontinuous phase takes place within each stage, of height $L_o$, to cause each droplet to have the same concentration. As a result, the dispersed

Table 3

Important Experimental Studies of Longitudinal Dispersion in Column-Type Extractors

| Type of Contactor | Reference |
|---|---|
| Spray Column | 4, 16, 17, 18, 22, 23, 29, 47, 64 |
| Packed Column | 6, 7, 11, 24, 26, 27, 34, 40 |
| Pulsed-Packed Column | 40 |
| Pulsed-Plate Column | 5, 12, 32, 37, 52, 56, 62 |
| Scheibel Column | 50 |
| Rotating-Disc Column | 36, 58, 59, 60 66, 67 |
| Oldshue-Rushton Column | 3, 19, 36, 37 |

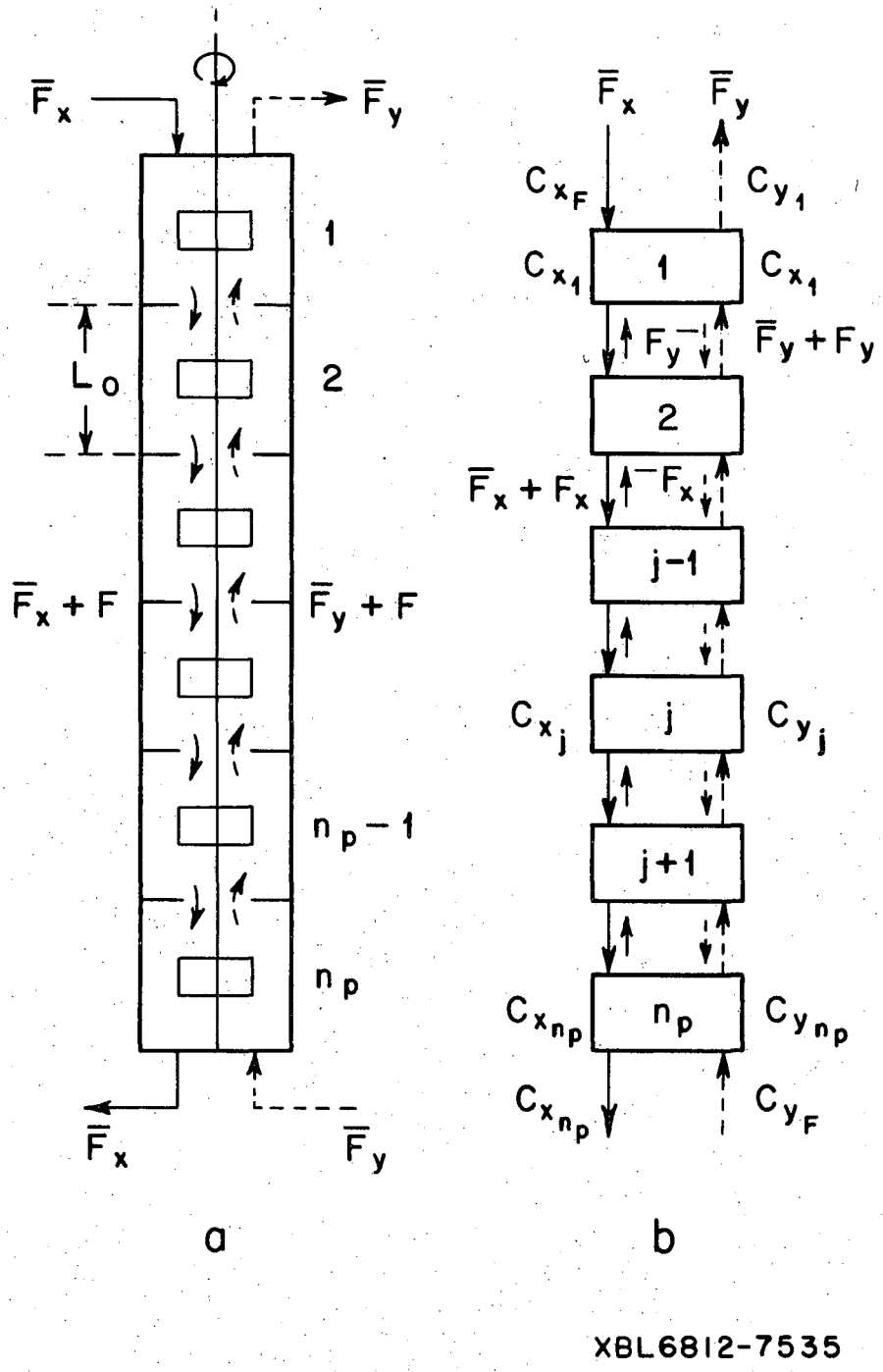


Fig. 4. Backflow model for countercurrent operation: (a) multicompartment contactor, (b) identification of flows.

phase behaves as a second continuous phase; $\bar{c}_y$ then represents the mean concentration of solute in the dispersed phase, and $c_x$ the mean concentration in the continuous phase, in each stage. For a constant overall mass-transfer coefficient, $k_{ox}$, interfacial area per unit volume, a, and a linear equilibrium, $c_x^* = b + mc_y$, the steady-state material balances for each phase around the jth stage are given by

$$\left[(\bar{F}_x+F_x)c_{x_{j-1}}+F_x c_{x_{j+1}}\right]-\left[(\bar{F}_x+F_x)c_{x_j}+F_x c_{x_j}\right]-\left[k_{ox}aL_o(c_{x_j}-c^*_{x_j})\right]=0 \tag{1}$$

and

$$\left[(\bar{F}_y+F_y)\bar{c}_{y_{j+1}}+F_y\bar{c}_{y_{j-1}}\right]-\left[(\bar{F}_y+F_y)\bar{c}_{y_j}+F_y\bar{c}_{y_j}\right]+\left[k_{ox}aL_o(c_{x_j}-c^*_{x_j})\right]=0 \tag{2}$$

The following dimensionless variables are now introduced:

$$\alpha_i = \frac{F_i}{\bar{F}_i}, \tag{3}$$

$$N_{oi} = \frac{k_{ox}aL_o}{\bar{F}_i}, \tag{4}$$

$$C_i = \frac{c_i}{c_x^o}, \tag{5}$$

$$X = \frac{C_x - (Q + m\,C_y^1)}{1 - (Q + m\,C_y^1)}, \tag{6}$$

$$Y = \frac{m\,(C_y - C_y^1)}{1-(Q+m\,C_y^1)} \quad , \tag{7}$$

where $Q$ is the constant, $b/c_x^o$, and $C_y^1$ denotes the dimensionless solvent inlet concentration. Equations (1) and (2) can therefore be written as

$$(1+\alpha_x)(X_{j-1} - X_j) - \alpha_x\,(X_j - X_{j+1}) = N_{ox}(X_j - \overline{Y}_j) \tag{8}$$

and

$$(1+\alpha_y)(\overline{Y}_j - \overline{Y}_{j+1}) - \alpha_y\,(\overline{Y}_{j-1} - \overline{Y}_j) = m\,N_{oy}(X_j - \overline{Y}_j) \quad . \tag{9}$$

The general solution to Equations (8) and (9) involves five variable parameters, and can be expressed in the form

$$X = X\,(\alpha_x, \alpha_y, N_{ox}, n_p, \Lambda) \tag{10}$$

and

$$Y = Y\,(\alpha_x, \alpha_y, N_{ox}, n_p, \Lambda) \quad , \tag{11}$$

where $\Lambda$ is a dimensionless capacity ratio, $m\overline{F}_x/\overline{F}_y$, and $n_p$ is the total number of stages. Vermeulen and co-workers (63) have summarized the types of solutions available for these equations. The backflow model seems particularly suited for the study of axial-mixing effects in agitated countercurrent extractors, such as the pulsed perforated-plate column, the rotating-disc column, and the Oldshue-Rushton column.

b. Diffusion Model

The second model for describing longitudinal dispersion in solvent-extraction columns is the dispersion model proposed by Miyauchi and Vermeulen (38) and also by Sleicher (54). It assumes that axial mixing in each phase can be described by a diffusional-type process represented by an axial-dispersion coefficient, E, which is superimposed on a plug-flow regime with mean velocity, F. The model further assumes that the dispersed phase behaves as a second continuous phase, rather than the actual situation in an extractor where the second phase remains dispersed in the form of droplets, as illustrated in Figure 5. Similar to the backflow model, the simplified representation is a valid approach when sufficient coalescence and redispersion of the discontinuous phase occur at each level in the column. The ideal and actual model become identical when there is no concentration fluctuation in the dispersed phase across the column cross-section.

The simplified model shown in Figure 6 depicts two-phase countercurrent flow with each phase undergoing longitudinal dispersion, and mass transfer occurring from phase X to phase Y. A steady-state material balance for each phase in a differential slice of the extractor, dz, leads to the equations:

$$\bar{E}_x \frac{d^2c_x}{dz^2} - \bar{F}_x \frac{dc_x}{dz} - k_{ox}a\,(c_x - c_x^*) = 0 \qquad (12)$$

and

$$\bar{E}_y \frac{d^2c_y}{dz^2} - \bar{F}_y \frac{dc_y}{dz} + k_{ox}a\,(c_x - c_x^*) = 0 \quad , \qquad (13)$$

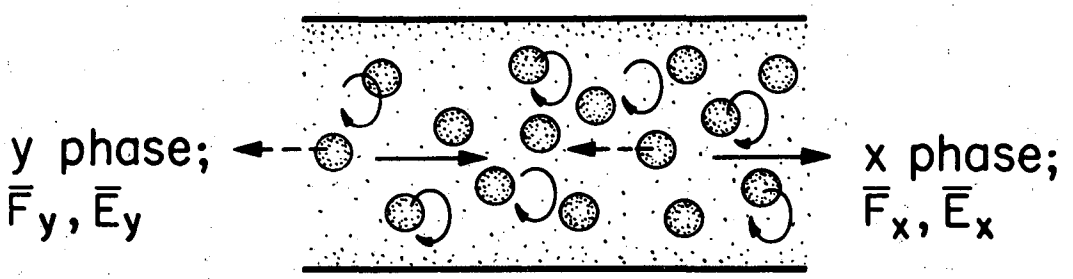


MU-14082-A

Fig. 5. Actual situation in an extractor.

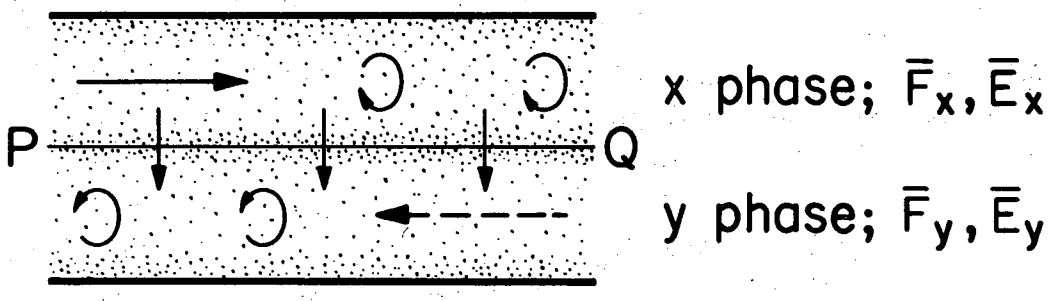


MU-14081-A

Fig. 6. Diffusion model for countercurrent operation.

where $\overline{E}_i$ is the superficial axial dispersion coefficient for phase i. Equations (12) and (13) can be written in the dimensionless form:

$$\frac{d^2C_x}{d\,Z^2} - P_xB\,\frac{d\,C_x}{d\,Z} - N_{ox}P_xB\left[C_x - (Q+m\,C_y)\right] = 0 \qquad (14)$$

and

$$\frac{d^2C_y}{d\,Z^2} + P_yB\,\frac{d\,C_y}{d\,Z} + N_{oy}\,P_yB\left[C_x - (Q + m\,C_y)\right] = 0\ , \qquad (15)$$

in which Z, $C_i$, $N_{oi}$, Q, and m have been previously defined, and where

B = dimensionless height, L/d,

d = characteristic local length, for instance, particle diameter ($d_p$) in packed beds, cm,

$l_i$ = effective mixing length, $\overline{E}_i/\overline{F}_i$, cm,

L = total column length, cm,

$P_i$ = local Peclet number, $d/l_i$, dimensionless, and

$P_iB$ = column Peclet number for phase i, $L\overline{F}_i/\overline{E}_i$, dimensionless.

Substituting the generalized concentrations, X and Y, given by Equations (6) and (7), and again introducing the extraction factor, $\Lambda = m\overline{F}_x/\overline{F}_y$, Equations (12) and (13) reduce to

$$\frac{d^2X}{d\,Z^2} - P_xB\,\frac{dX}{dZ} - N_{ox}P_xB(X - Y) = 0 \qquad (16)$$

and

$$\frac{d^2Y}{d\,Z^2} + P_yB\,\frac{dY}{dZ} + \Lambda N_{ox}P_yB(X - Y) = 0\ . \qquad (17)$$

Numeric and analytic solutions to the above set of linear second-order differential equations have been reported by Sleicher (54) and by Miyauchi, McMullen and Vermeulen (33, 35, 38). The general result is in the form

$$X = X\,(N_{ox},\ \Lambda,\ P_xB,\ P_yB,\ Z) \quad , \tag{18}$$

$$Y = Y\,(N_{ox},\ \Lambda,\ P_xB,\ P_yB,\ Z) \quad . \tag{19}$$

The $Z$ values of most interest, at the ends of the column, are $0$ and $1$. Miyauchi and Vermeulen (35, 38) have also presented analytical solutions for special cases obtained by simplifying the basic equations. Applications of their use to specific types of apparatus are also indicated. Theoretically the diffusion model is more appropriate for unstaged contactors, such as packed and spray columns. However, for long columns ($N_{ox} \gg 1$ or $n_p \gg 1$) the diffusion model and the backflow model are relatively interchangeable (39).

# II. STATEMENT OF THE PROBLEM

## A. Experimental Objectives

The purpose of the present study is to develop a new type of countercurrent solvent-extraction column which (1) provides for a high degree of mass transfer; (2) minimizes the effect of longitudinal dispersion; and (3) has no internal moving parts. High rates of mass transfer usually require mixing patterns of sufficient intensity to subdivide and circulate the dispersed-phase droplets without forming a stable emulsion. Certain column-type extractors, such as pulsed-plate and rotating-shaft columns, meet these criteria while providing many "transfer units" (or many "theoretical stages"). Longitudinal dispersion is reduced in these types of columns by compartmentalizing the flow, as discussed in Section I-A. Other desirable features on which the choice of extractor design can be based include high capacity, simplicity in construction, reasonable construction and operating costs, and relatively precise scale-up.

## B. Concept of a Jet-Mixed Column

A jet-mixed extraction column (JMC), which is believed to fulfill the design objectives, is currently under development in this laboratory. The JMC contains several stages of two coaxial tubular perforated rings, the inner and outer ring at each level being connected through a small centrifugal pump outside the column. Small horizontal uniformly spaced ports are drilled around the inside of the large rings and the outside of the small rings, to permit flow into or out of each ring.

At each stage, liquid is continually withdrawn from the column through the ring connected to the low-pressure side of the pump (intake ring), and re-emitted into the column through the ports of the opposite ring (jetting ring). The cross flow at a ring-level may be directed inward or outward. Since the fluid is subjected to high shearing forces when passing through the centrifugal pump, it is important to recirculate only the continuous phase to avoid forming stable colloidal dispersions. Superimposing the radial flows at each stage on the countercurrent flow of the continuous and dispersed phases, the resultant vortex patterns produced in each compartment are shown schematically in Figure 7.

The JMC provides for nearly uniform, controllably fine dispersion of the discontinuous phase. The effect of longitudinal dispersion is reduced by both the position and the action of the rings; the rings tend to compartmentalize the flow, while the radial jetting gives a nearly uniform concentration across any one cross-section of the column.

The internal design of the JMC contributes several other important advantages. Because void volume is high, relatively large throughputs can be attained. Also, since there are no moving parts within the column, maintenance costs are kept low. If a pump fails it can be externally disconnected and quickly replaced, thereby minimizing shut-down time. This type of unit should be well suited for shielded nuclear installations.

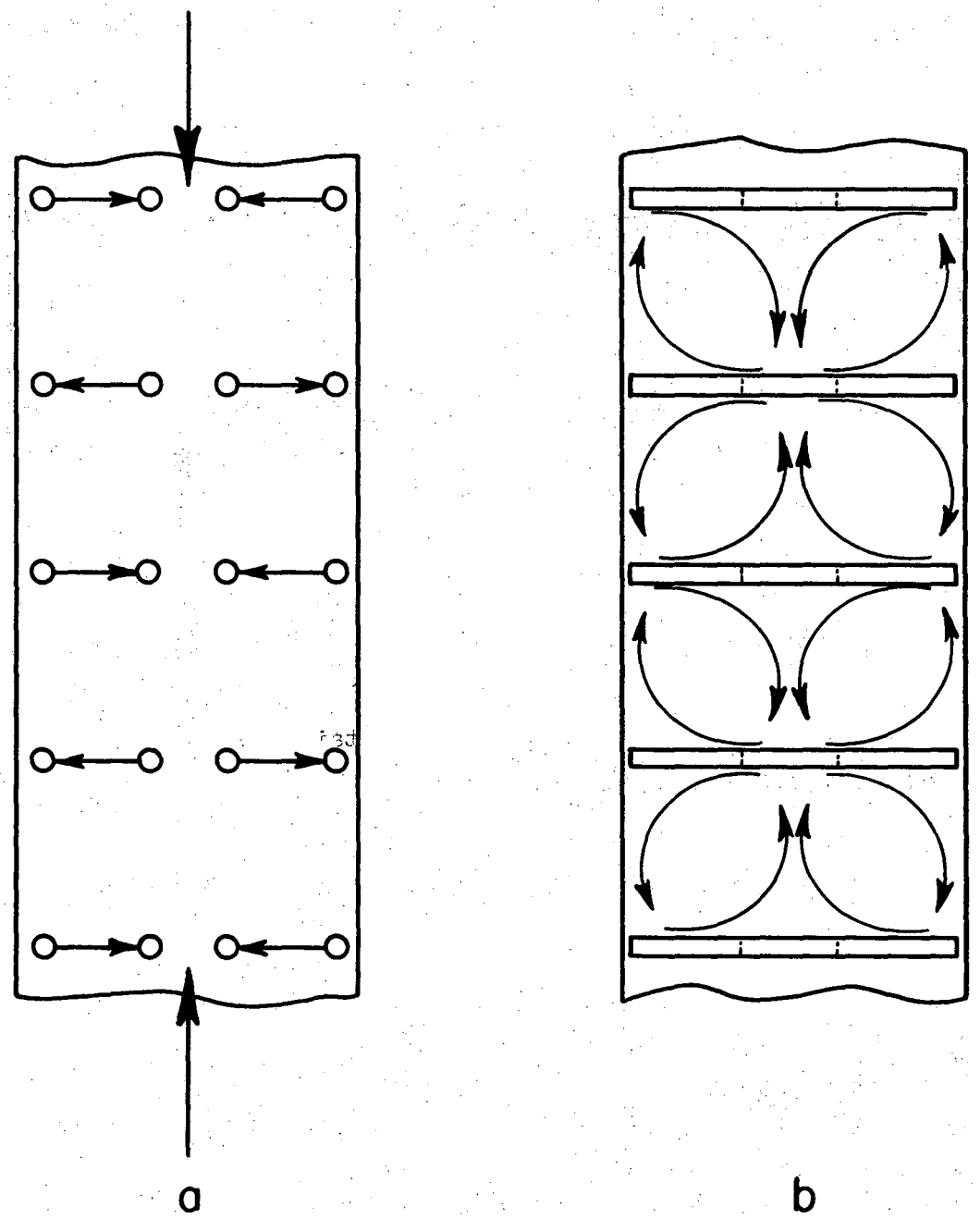


Fig. 7. Resultant vortex patterns in the jet-mixed column.

# III. APPARATUS

## A. Column Body

The column body shown in Figure 8 is fabricated from a 24-in. length of 6-in.-o.d. cast acrylic tubing with a 1/4-in.-wall thickness. Acrylic plastic is relatively transparent, allowing interstage mixing patterns to be visually observed and photographed. Also, it has a relatively high tensile, compressive, and flexural strength, making it easy to attach and position the intake and jetting rings. Nine pairs of 1/2-in.-dia. holes were drilled at 1-in. intervals along the column length, with 45° spacing between inlet- and outlet-ring connections at each level. Figure 9 shows an exploded assembly of one of the column fittings which permits the insertion of a 1/2-in. stainless-steel connecting tube into the column. At those holes not being used for radial circulation lines, the drilled tail-piece fittings are replaced with tailpiece plugs. Only three stages of ring assemblies have been tested during the present study, with stage heights varying from 1 to 8 inches. With the design described, repositioning of the rings has proven to be simple and rapid.

The choice of a plastic column does restrict the types of solvents that may be investigated. Acrylic plastic is soluble in ketones, esters, and aromatic and chlorinated hydrocarbons, although unaffected by aqueous acids or alkalies. Aliphatic hydrocarbons and alcohols (such as isodecane and 2-ethyl hexanol), along with water, have been used without damage to the apparatus.

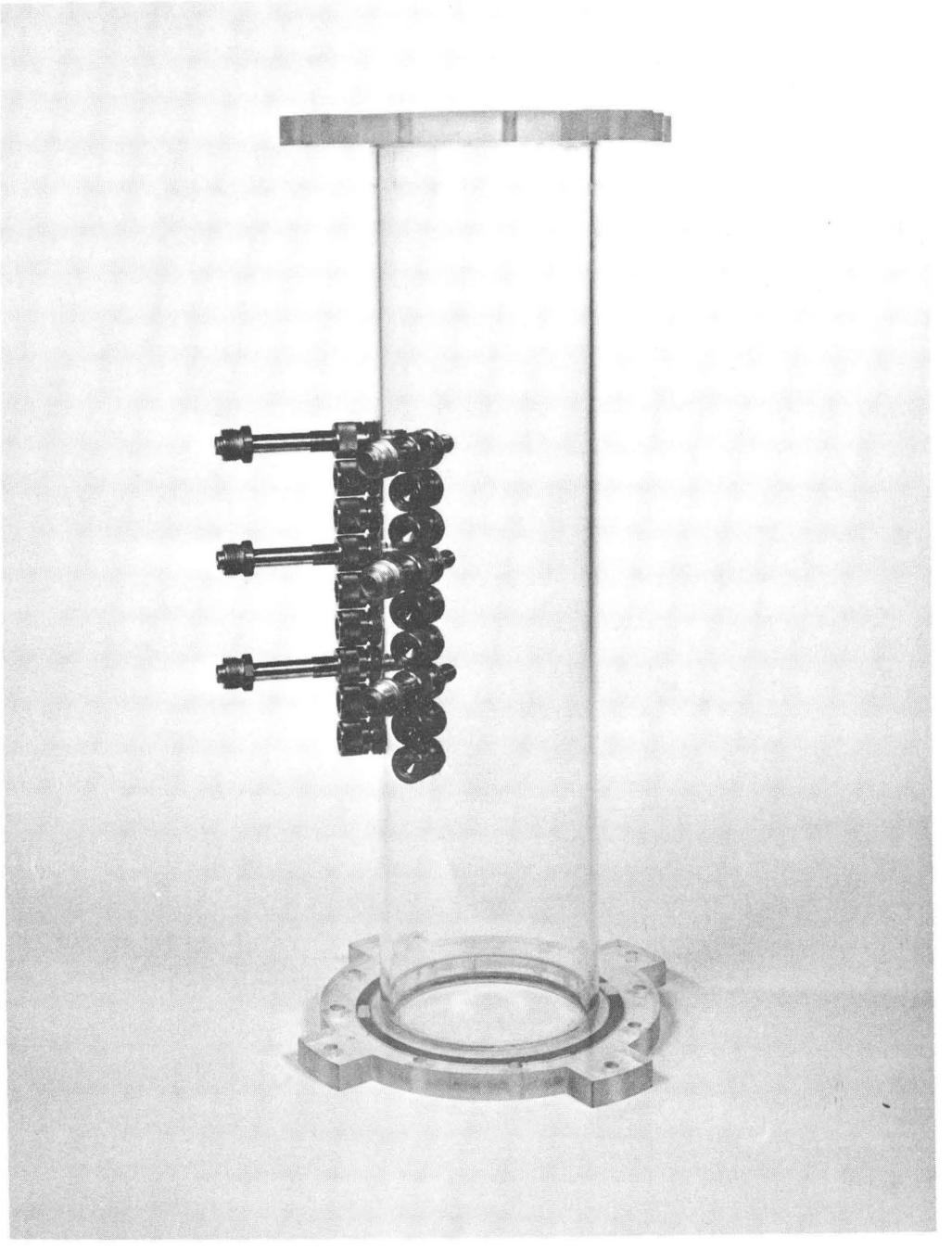

XBB 6812-7360

Fig. 8. Column body before assembly.

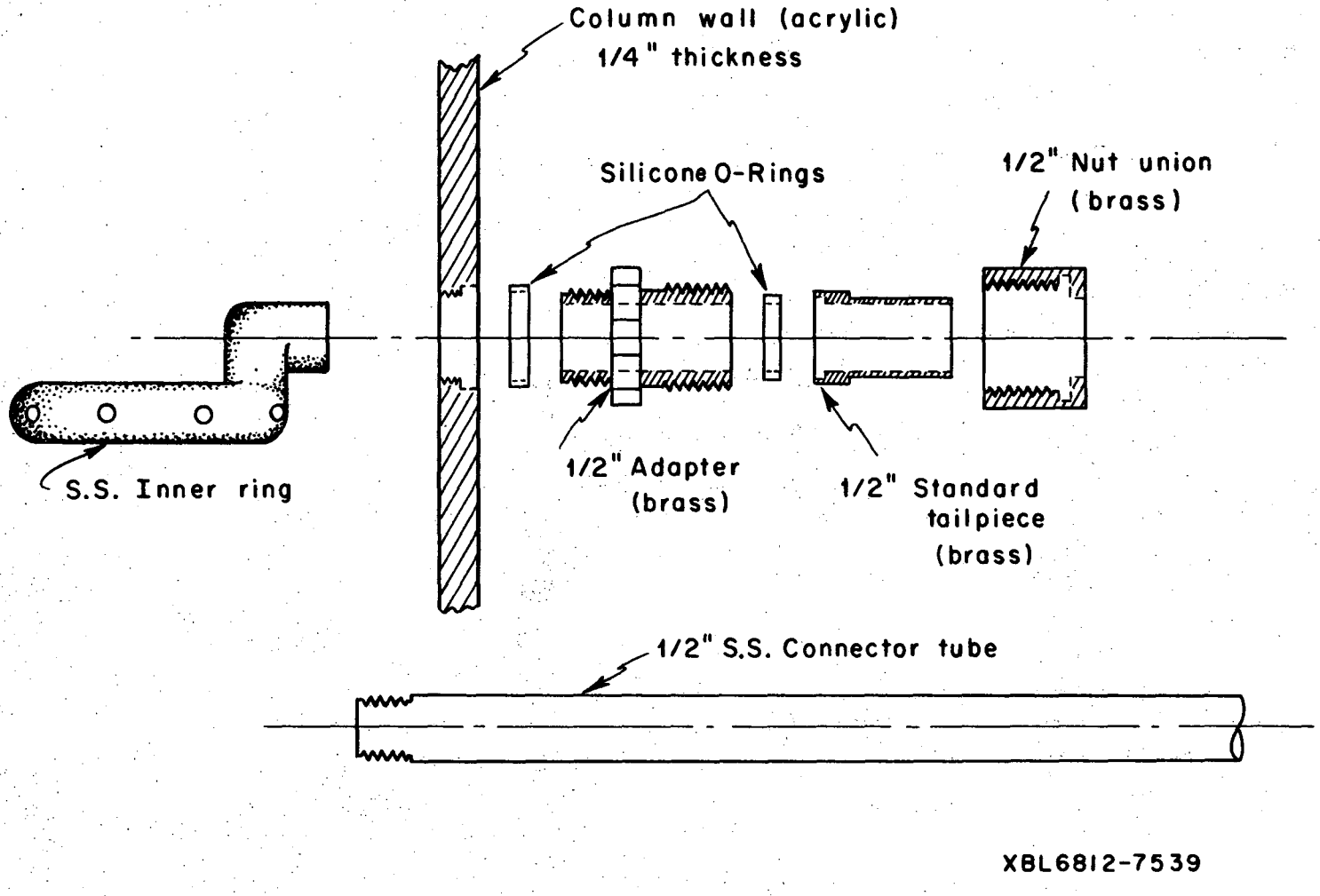


Fig. 9. Exploded assembly of column fitting .

## B. Column Heads

Expanded aluminum end-sections, used in previous extraction studies by Jacques (27) and Moon (40), were bolted above and below the column (see Figures 10, 11, and 12). Since the column was designed to operate with either the light or the heavy phase dispersed, the same construction was used for both upper and lower heads. Fittings included two 2-1/8-in.-dia. pyrex glass windows for visual observations, a 6-in. inlet distributor nozzle, two symmetrically placed outlets, and two Teflon-coated liquid-level probes for two-phase experiments (shown schematically in Figure 11 as a single probe). O-rings made of natural rubber provided a leak-proof seal between the plastic column and the metal heads, while Viton O-rings were used for the head flanges and windows. To prevent corrosion and reduce contamination, the inside surface of each aluminum head and cover plate was coated with a white epoxy paint.

Special consideration was given to the design of the inlet nozzle for the discontinuous phase (27) (see Figure 13). A uniform drop size was desired in order to achieve a velocity profile as flat as possible. According to Johnson and Bliss (28), the injection velocity should be maintained between 1000 and 1500 ft/hr. The distributor nozzle was therefore designed with a set of removable injection plates containing 0.10-in.-dia. inlet holes, varying in number (from 19 to 169) to provide for a wide range of flow rates.

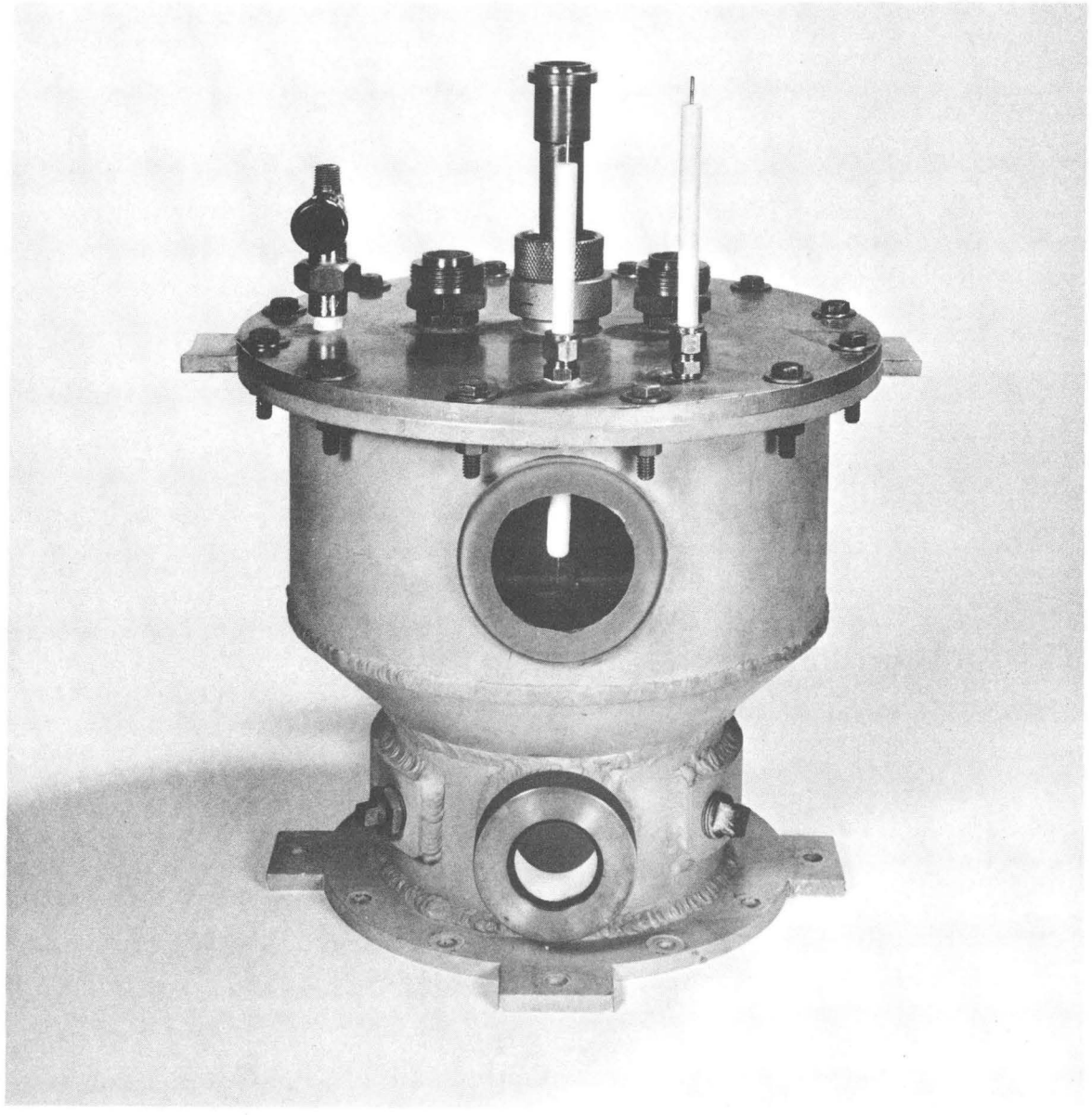

XBB 6812-7370

Fig. 10. Photograph of column head.

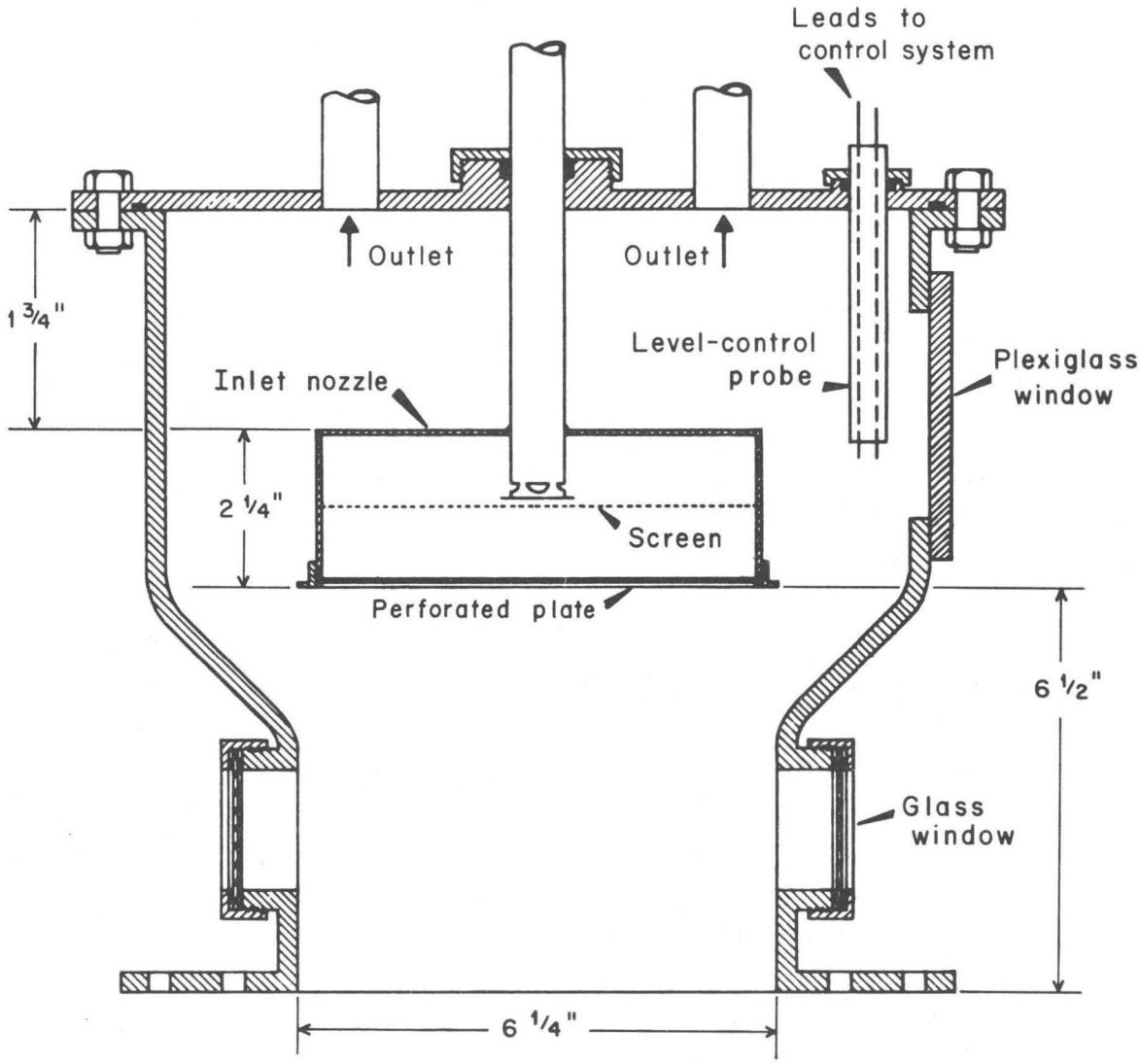


Fig. 11. Diagram of column head.

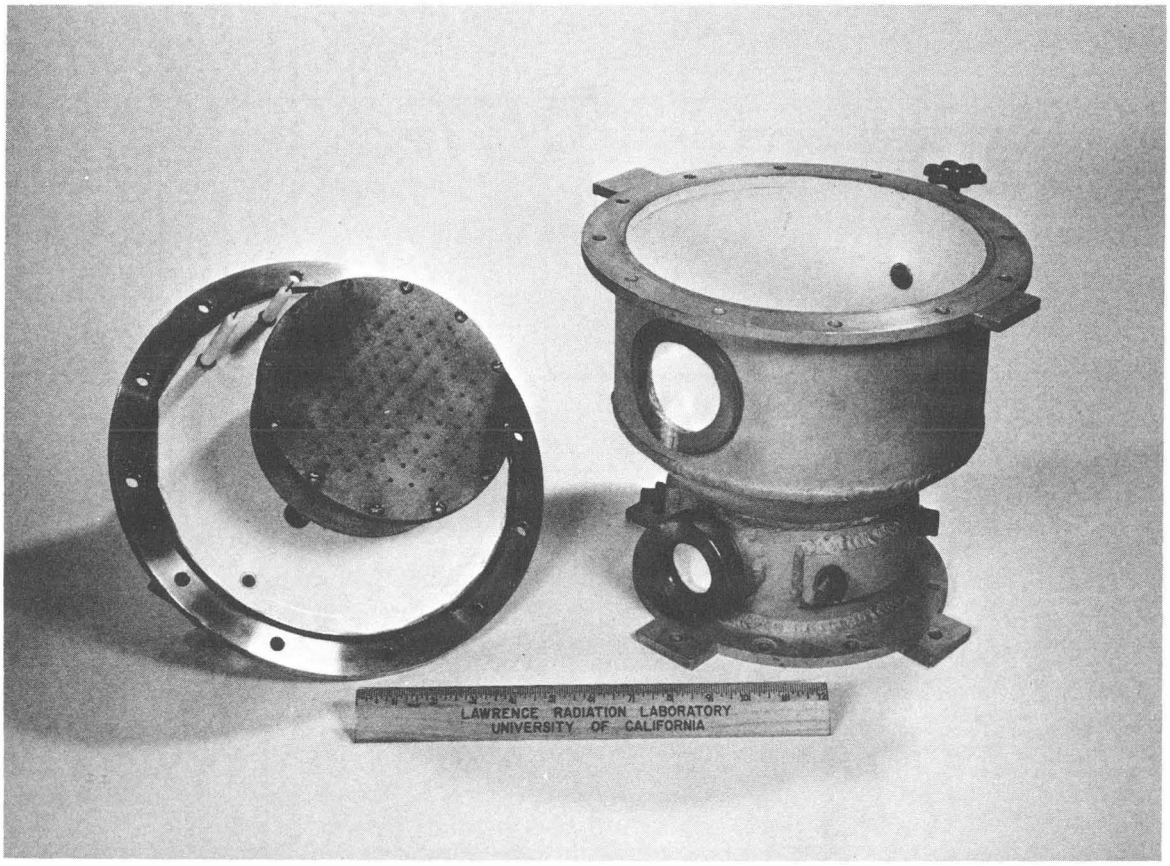


XBB 6812-7369

Fig. 12. Column head and flange plate.

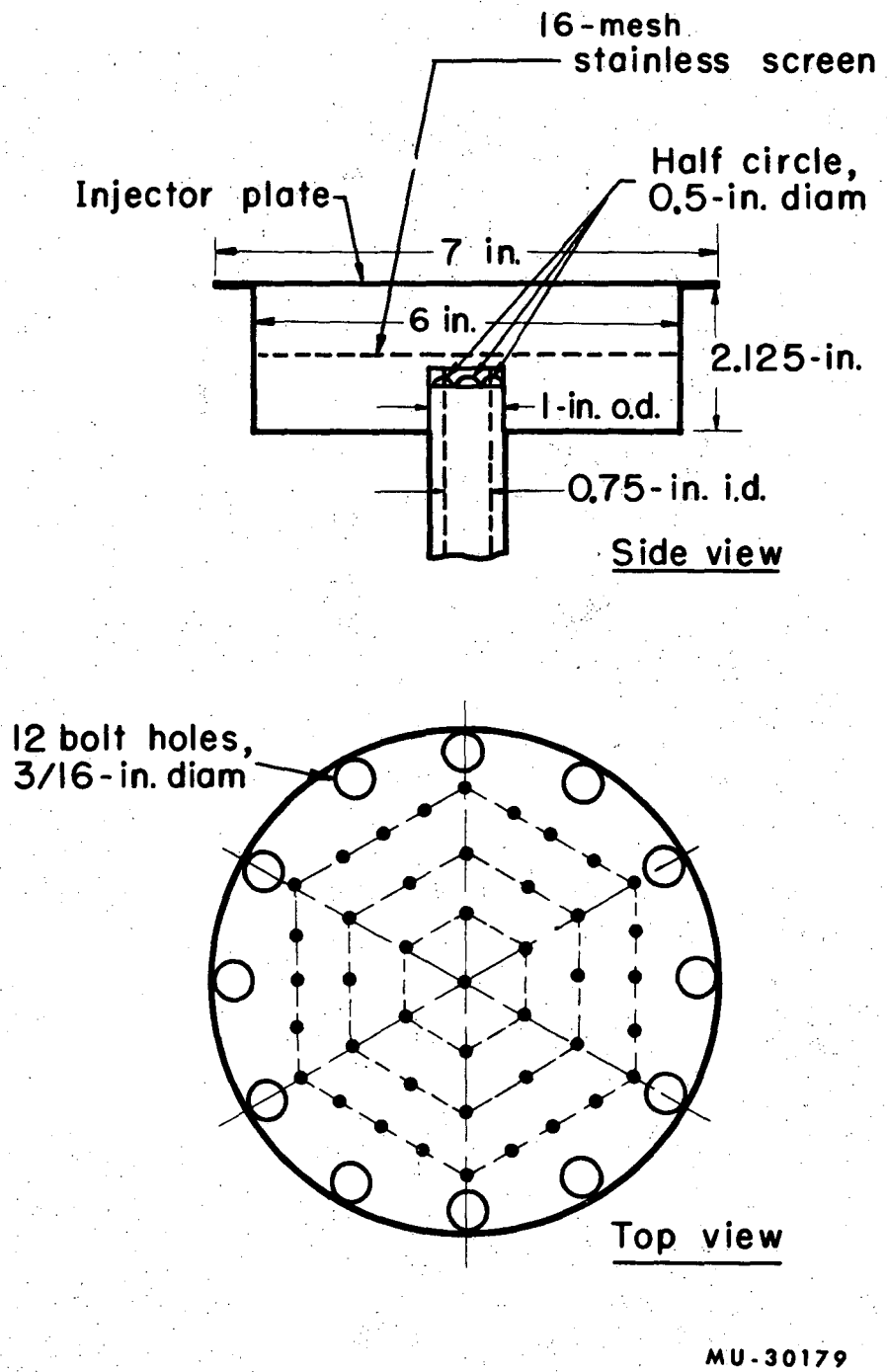


Fig. 13. Detail of nozzle construction .

## C. Rings

Each pair of rings was formed from 3/8-in.-o.d. stainless-steel tubing with 0.049-in. wall thickness (see Figure 14). The outside diameters of the inner and outer ring are 1.875 inches and 5.25 inches, respectively. Prior to welding, each ring-stem was separately machined from a 1-in. stainless-steel block, and drilled to accomodate a 1/2-in. threaded connecting tube. Each stem outlet projects 1/2 in. out of the plane of the ring, to provide space between the outer ring and the connector tube of the inner ring. For the outer rings, welding the machined stem to the inner side of the ring made it possible to reduce the clearance between the ring and the column wall to 1/16 in., and thus prevent serious wall effects. The top view of a ring-stage fastened to the column body is shown in Figure 15.

Detailed design criteria for selecting the size and distribution of the ring ports will be developed in Section IV.

## D. Pumps and Tubing

Radial circulation at each ring-stage was provided by an Eastern Industries model B-1 centrifugal pump (115 volts ac-dc, 1/20 hp), delivering up to 1.5 gal/min. The three pumps used in the present work were mounted on a plywood panel next to the column, each at the same level as its respective ring-stage. The pumps were connected to the outer fittings of the column by 3/8-in.-o.d., 1/4-in.-i.d. polyethylene tubing, chosen for being inert to the solvent systems employed, and flexible enough to accomodate changes in stage spacing.


XBB 6812-7364

Fig. 14. Inner and outer rings.

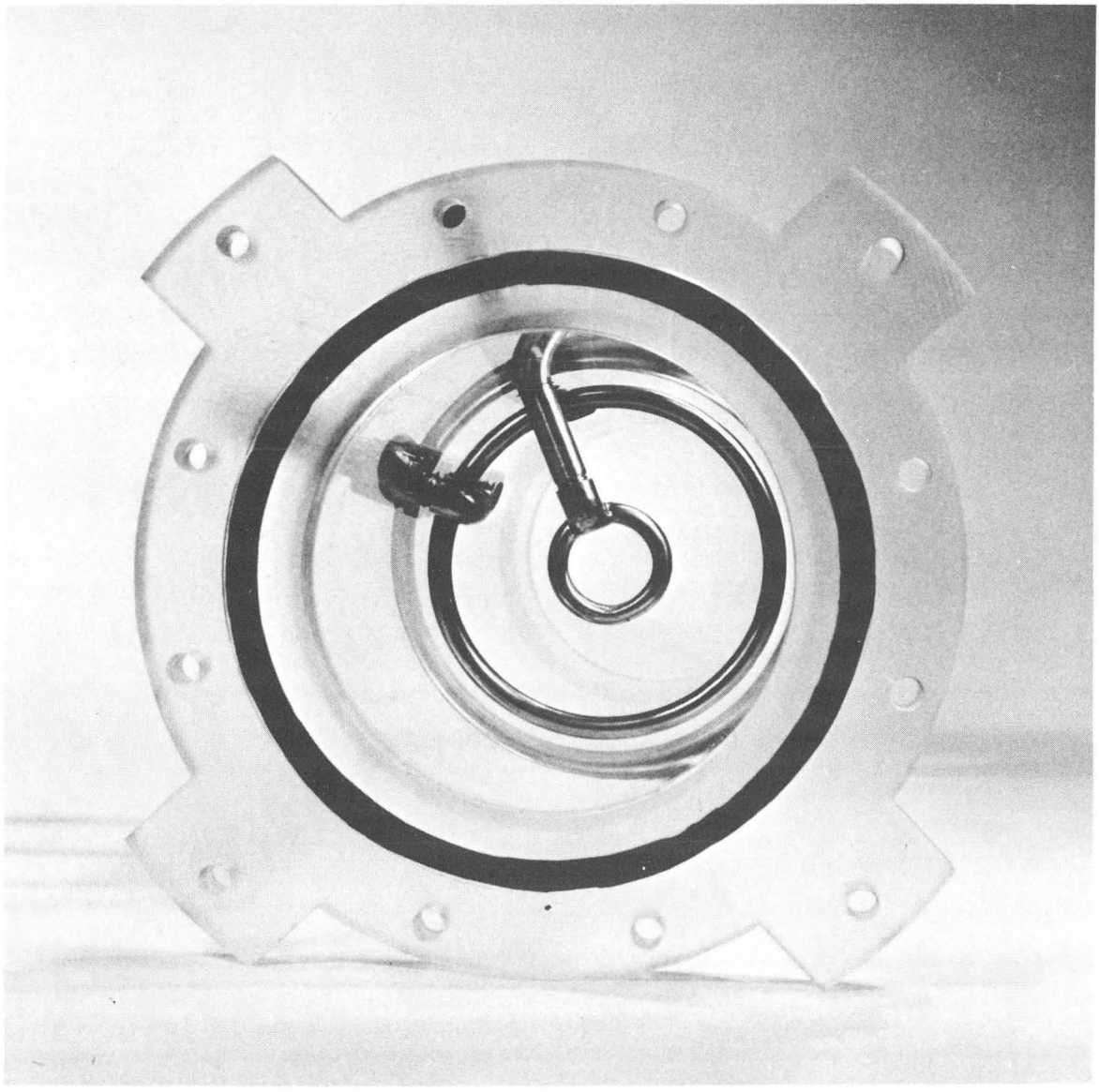

XBB 6812-7361

Fig. 15. Top view of a ring stage.

It is important to maintain equal radial flow rates at each stage, and to have accurate knowledge of these flows. Variable transformers (Superior Electric "Powerstats") connected to the pumps provided flow control at circulation rates between 0.2 and 1.5 gal/min. By shifts in tubing connections, a calibrated rotameter (1.52 gal/min at 100% maximum flow) on the panel board could be inserted between the pump outlet and the jetting ring of any desired stage, and calibration curves of flow rate vs. Powerstat setting developed for each pump.

E. Liquid-Interface Level Control

The interface could be maintained at the top or the bottom of the column, so as to make the water phase either continuous or dispersed. Coarse adjustment of the interface was accomplished by raising or lowering the inverted-U leg of the exit water line, as shown in the piping diagram of Figure 16. A globe valve in the exit water line served as a fine adjustment.

To indicate the position of the interface, two Teflon-coated nickel-rod probes were mounted in each head section. The probes were slightly staggered in level to provide a neutral zone. Probe leads were connected to an electronic circuit which was constructed to give a maximum closed-circuit current of 1 ma. Various current readings could be obtained, depending upon the position of the interface relative to the probe tips. However, use of conductivity to estimate the interface level was unsatisfactory, mainly because the liquid-liquid interface was

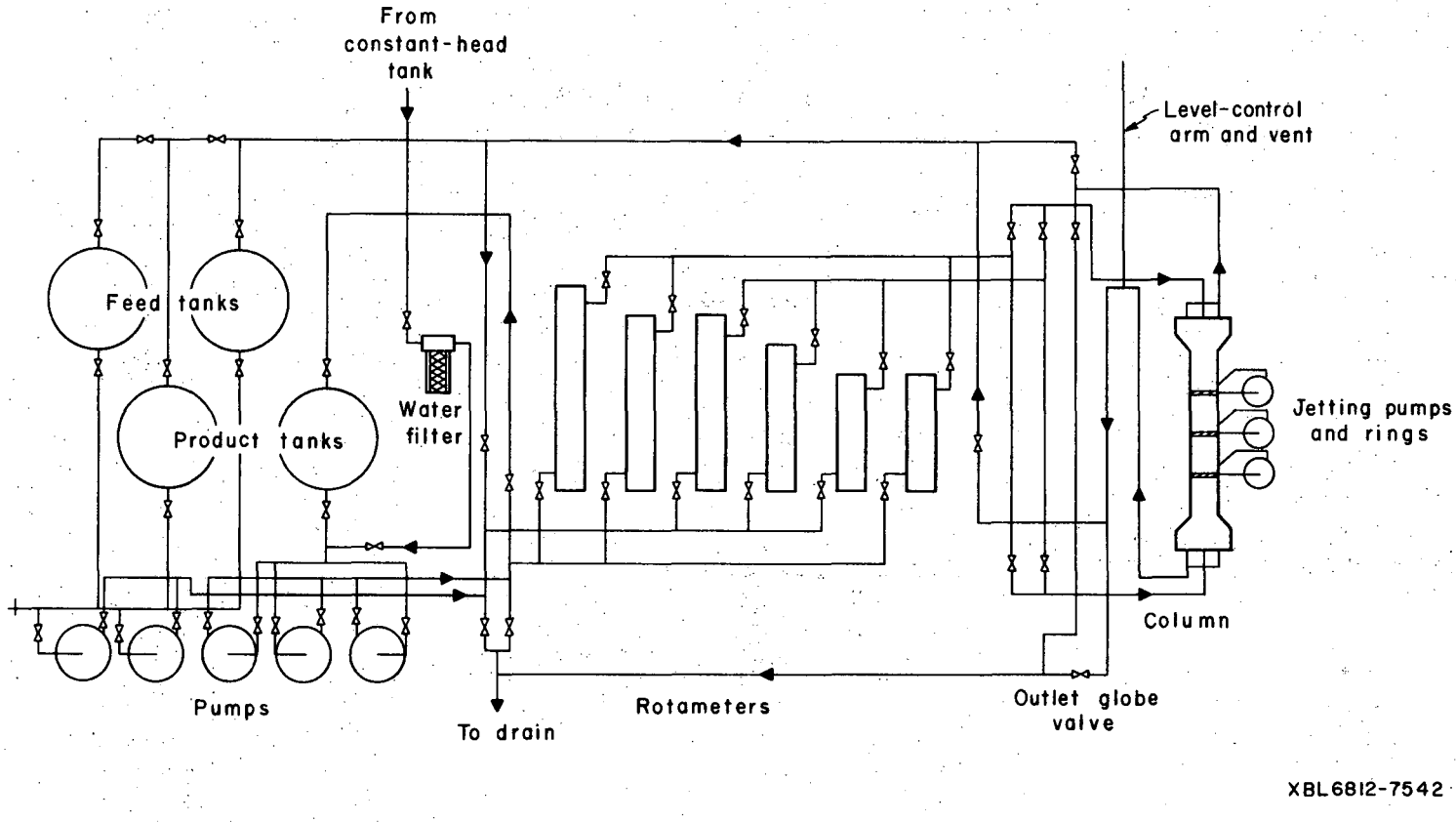


Fig. 16. Layout of flow system.

not always sharp and distinct. Hence it was decided not to use a solenoid valve in the outlet water line.

As an alternative, the interface could be controlled manually if it could be observed visually. Therefore a 2-1/2-in. hole was drilled in the upper head, and a 3-1/4-in. Plexiglass "window" was glued to the aluminum surface by epoxy resin. With this addition, it was possible to maintain the liquid-liquid interface in the upper head within narrow limits by manual adjustments of the exit globe valve.

F. Piping Arrangement and Storage Facilities

The complete flow arrangement is shown in Figure 16. The organic phase was piped from 55-gal. storage drums by means of centrifugal pumps. Water for the experiments was supplied under gravity flow from a 150-gal. constant-head tank mounted on the roof of the building, about 50 feet above the column. The product organic phase was returned to the supply tanks through an overhead line, and product water was drained to the sewer.

The incoming aqueous and organic flows were manifolded and valved, in order to meter each of them through the appropriate unit in a bank of six rotameters. The rotameters were calibrated by volume flow of water. Organic flow rates were corrected by assuming that equal-weight flow rates gave equal readings, and by using standard correction charts by the Fisher-Porter Company. The working ranges of water flow through the six rotameters were 0 to 40 gal/min, 0 to 6 gal/min, 0 to 1.5 gal/min, (2) 0 to 0.8 gal/min, and 0 to 0.3 gal/min.

# IV. RESULTS OF EXPERIMENTAL TRIALS

## A. Single-Phase Flow

### 1. Ring Design

#### a. Initial Design Criteria

The primary objective in setting the size, number, and location of the ring ports has been to maintain substantially uniform flow through each ring . A second aim has been to provide sufficiently intense jetting action to subdivide dispersed-phase droplets and increase their overall mass-transfer coefficient. Two types of stage configuration were possible in the present design. In the first type, designated as IRJ-ORW, the jetting fluid emanates from the inner ring after being withdrawn through the outer ring. The second type, referred to as ORJ-IRW, involves flow in the opposite direction.

It was recognized at the start that a more uniform flow would result through all the ports, assuming these to be of equal diameter, if the resistance to flow at the ports exceeded the resistance inside the tubular ring. Accordingly, the ratio of the total port area in each ring to the inner cross-sectional area of the tubular ring was not to exceed unity:

$$\frac{\sum A_P}{A_t} \leq 1 \qquad (20)$$

Since

$$A_t = \frac{\pi}{4}\left[0.375\text{-}2(0.049)\right]^2 = 0.060 \text{ in}^2 ,$$

$$\sum A_p \leq 0.060 \text{ in}^2 .$$

In order to improve the uniformity of the jetting action by a nearly equal spacing of ports, twice as many ports were provided in the outer ring as in the inner ring. The initial holes were drilled on a 22.5° spacing around the inside diameter of the outer ring and on a 45.0° spacing around the outside diameter of the inner ring. Table 4 summarizes these design values.

Table 4

Initial Ring Design

| Configurations | Number of Ports | Port Diameter (in) | Total Cross-Sectional Area of Ports ($in^2$) | $\frac{\sum A_p}{A_t}$ |
|---|---|---|---|---|
| IRJ, IRW | 8 | 3/32 | 0.055 | 0.92 |
| ORW, ORJ | 16 | 1/16 | 0.049 | 0.82 |

b. Flow-Distribution Analysis

Flow distributions in "blowing" and "sucking" manifolds have been discussed by Acrivos, Babcock, and Pigford (1), who have shown that equal rates of flow can generally not be obtained from identical ports. When a fluid stream is divided into parts by means of a manifold, changes in fluid pressure occur due to wall friction and to the changing fluid momentum. While friction causes the pressure to fall in the direction of flow, the sudden changes in direction of the portion of fluid flowing through each port results in a local pressure rise in a blowing manifold, and a local drop in a sucking manifold. Acrivos et al. present a

one-dimensional theory for the division of a fluid into parts within a straight manifold, and give design charts for estimating rapidly the nonuniformity of flow.

A series of experiments were performed with the IRJ-8 ring (see Table 4) to examine the flow uniformity. Using water as the fluid medium, the velocity profile around the ring was determined by collecting the flow into air through each port, during timed intervals. Figure 17 shows the results of these experiments for several inlet flow rates. At approximately 1 gal/min, the experiments gave a 46% higher flow from the outer-most ports (4 and 5) than from the first ports (1 and 8), while the design charts based upon Acrivos's theory predicted only a 6% difference for this ratio. In calculating the latter value, the ring was modelled as a straight tube equivalent in length to one-half the mean ring circumference. The discrepancy seems due to the fact that parallel flow in the tubular ring is not established.

Several applicable conclusions are obtained from Acrivos's article:

(1) In a sucking manifold, the friction and momentum effects occur in the same direction, creating the lowest pressure and hence the maximum flow at the port nearest the open end. These effects oppose one another in a blowing manifold, and the location of maximum and minimum flows depends upon the system variables.

(2) To obtain a uniform pressure distribution along a manifold with identical ports, it would be necessary to construct one with a gradually

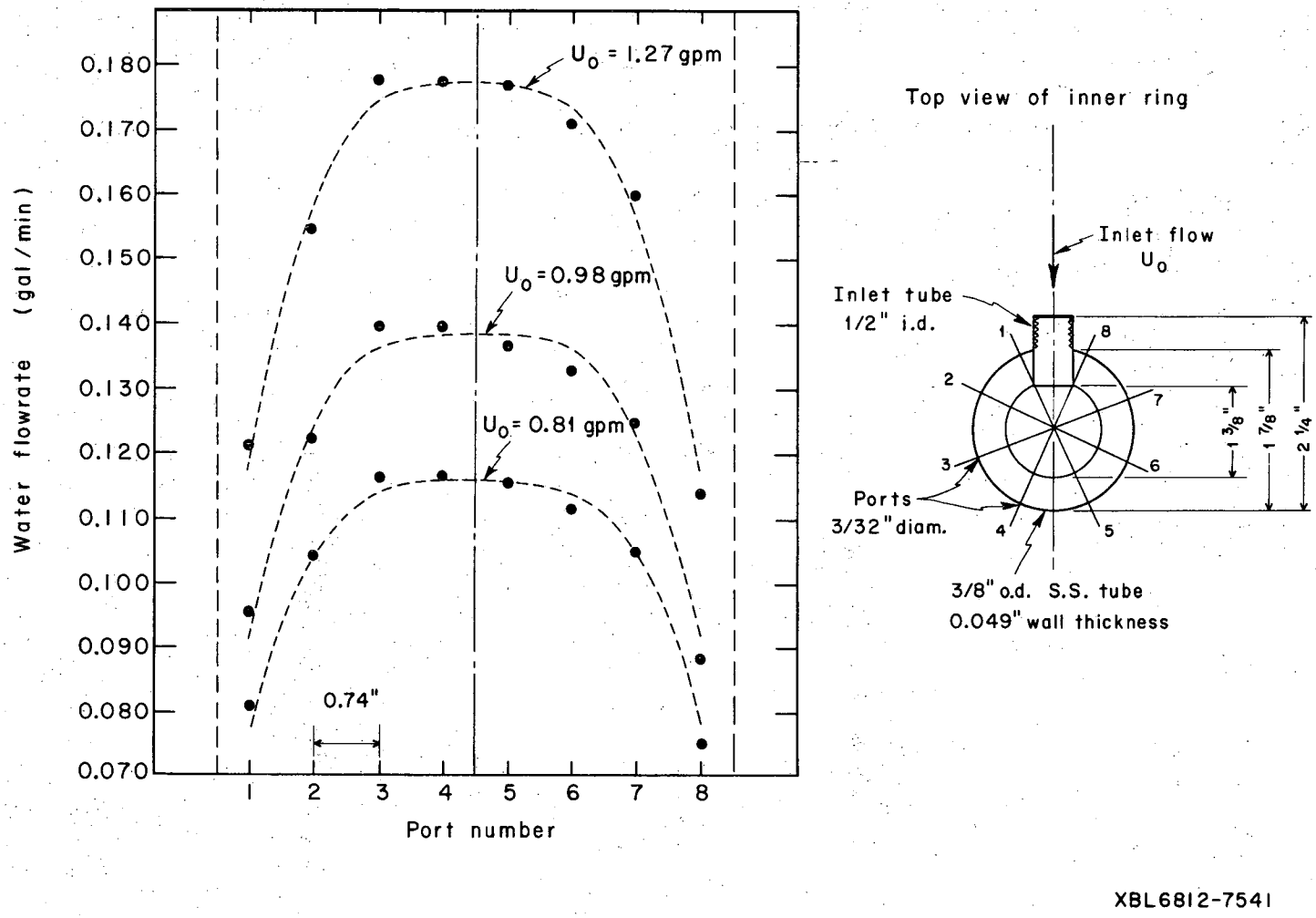


Fig. 17. Flow distribution around a jetting ring.

decreasing cross-sectional area, so as to keep the fluid velocity fairly constant while the mass flow rate decreased. Such a design is not very practical, chiefly because a manifold designed to provide identical flows through all ports at one main flow rate generally does not give identical flows at another main flow rate.

In the present work, an inequality in flow through the ring ports will be accepted, provided there is sufficiently strong jetting action from each port to insure adequate radial flow across the column.

(3) For substantially uniform flow in a straight tubular manifold, Equation (20) should apply. In the case of a circular manifold where the flow divides, half the total port area should be compared with the manifold cross-section. For the intake and jetting rings in the present work, the limiting-port-area criterion was revised to be:

$$\frac{\sum A_p}{A_t} \leq 2 \qquad (21)$$

Based upon this requirement, the intake rings were modified by drilling 15 additional 1/16-in.-dia. holes uniformly around the outer rings and 8 additional 3/32-in.-dia. holes around the inner rings. The number of jetting ports were not increased because it appeared that satisfactory jetting action could be obtained using the initial criterion. The modified ring-port design is given in Table 5.

Table 5

Modified Ring Design

| Configuration | Number of Ports | Port Diameter (in) | Total Cross-Sectional Area of Ports ($in^2$) | $\frac{\sum A_p}{A_t}$ |
|---|---|---|---|---|
| IRJ | 8 | 3/32 | 0.055 | 0.92 |
| ORW | 31 | 1/16 | 0.095 | 1.58 |
| IRW | 16 | 3/32 | 0.110 | 1.83 |
| ORJ | 16 | 1/16 | 0.049 | 0.82 |

c. Radial-Flow Limitations

Following these changes, the column was reassembled at a 4-inch stage spacing, with the IRJ-ORW configuration at stages 1 and 3 and the IRW-ORJ design at stage 2. After filling the column with water at a continuous-phase flow rate of 0.8 gal/min, each radial line was purged to release entrapped air prior to operation. The radial pumps were subsequently started and observations were made at various radial flow rates. Flows greater than 1 gal/min tended to create an excessive amount of small air bubbles throughout the column. If the pumps were started slowly and gradually increased to somewhat less than 1 gal/min, a small but tolerable amount of bubbles was formed. Varying the continuous-phase flow rate did not affect this result. It was concluded that the air bubbles originate from dissolved air in the feed water, and are released

in the intense mixing created by the jetting rings. The problem has been partially solved by restricting radial flows to less than 1 gal/min. A further reason for this restriction, pointed out in Section IV-B, is that high radial flow rates initiate the formation of stable emulsions (during two-phase flow operations).

2. Dye-Injection Studies

a. Apparatus

By injecting a water-soluble dye (bromophenol blue) upstream of a jetting manifold during single-phase flow operation, and observing the resultant mixing patterns, the qualitative effects of varying stage configuration, stage spacing ($h_c$), and radial and longitudinal flow rates ($F_r$ and $F_c$, respectively) were determined. Dye was injected from a 250-cc Erlenmeyer flask fitted with a two-holed rubber stopper, into which two lengths of 1/4-in.-o.d. polyethylene tubing were inserted. One tube was connected to a compressed-air source, while the other served as the dye outlet and was connected directly into the desired circulation line by means of a polyethylene tee fitting and a 3/8-in. stainless-steel Hoke valve.

b. Effect of a Central Cylindrical Wall

Initial dye-injection tests revealed that longitudinal dispersion was being increased along the axis of the column. As shown schematically by the arrows in Figure 18a, dye solution flowed rapidly downward (in excess of $F_c$) through the inner rings of each stage, essentially unaffected by the adjacent vortex patterns. Regardless of stage

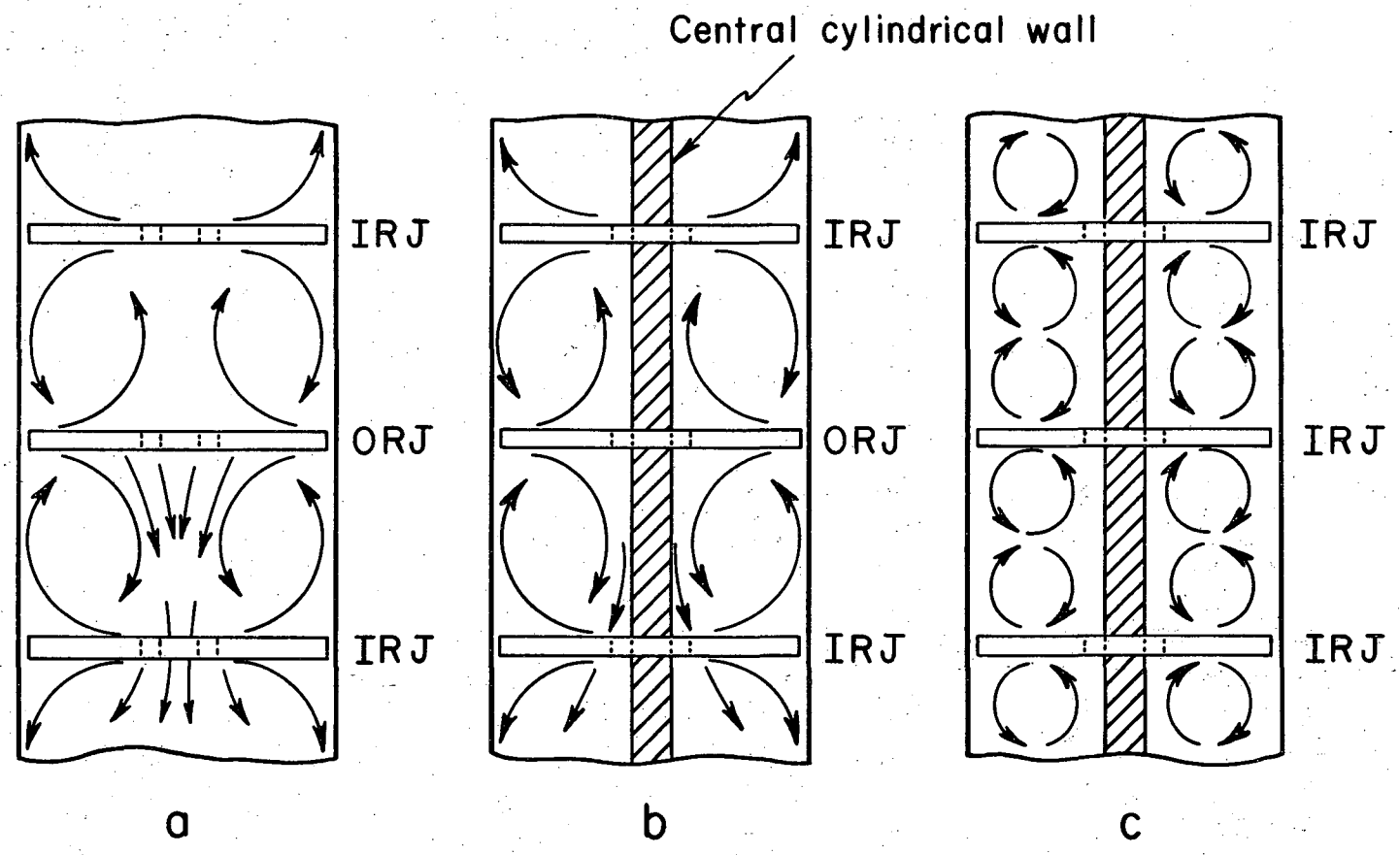


Fig. 18. Schematic of continuous-phase mixing patterns in the jet-mixed column .



UCRL-18679

position, the ORJ-IRW configuration contributed in large measure to the observed "downdrafting". To eliminate this undesirable effect, a central cylindrical wall, in the form of a 20-in.-long 1-1/4-in.-dia. Lucite rod, was snugly inserted through the inner rings, as illustrated in Figure 19. To position the plastic rod, a stainless-steel pin was placed through the center of gravity of the rod and supported by the inner ring at stage 2.

The addition of a central cylindrical wall was highly effective in reducing axial dispersion, as evidenced by the more localized mixing patterns in the column (see Figure 18b and c). Although the ORJ-IRW stage configuration continued to permit dye to surge downward adjacent to the Lucite wall, this occurred to a smaller and more tolerable extent. No "downdrafting" was observed when the IRJ-ORW configuration was used at every stage, where two vortex rings were now produced in each stage.

Dye-mixing photographs in the IRJ-ORW configuration, taken at 1, 3, and 5 seconds following a one-second dye injection, are given in Figure 20. Although the mixing patterns are not clearly discernible, due to the increased amount of dye that was necessary to produce more contrast, the symmetry and localization of the flow can be observed.

c. Effect of Stage Spacing

As stage spacing ($h_c$) was increased from 2 to 8 inches, the vortices produced between stages also became progressively larger. Because one aim of the JMC is to reduce backmixing, a small $h_c$ is desirable. In the present work, with the IRJ-ORW configuration at

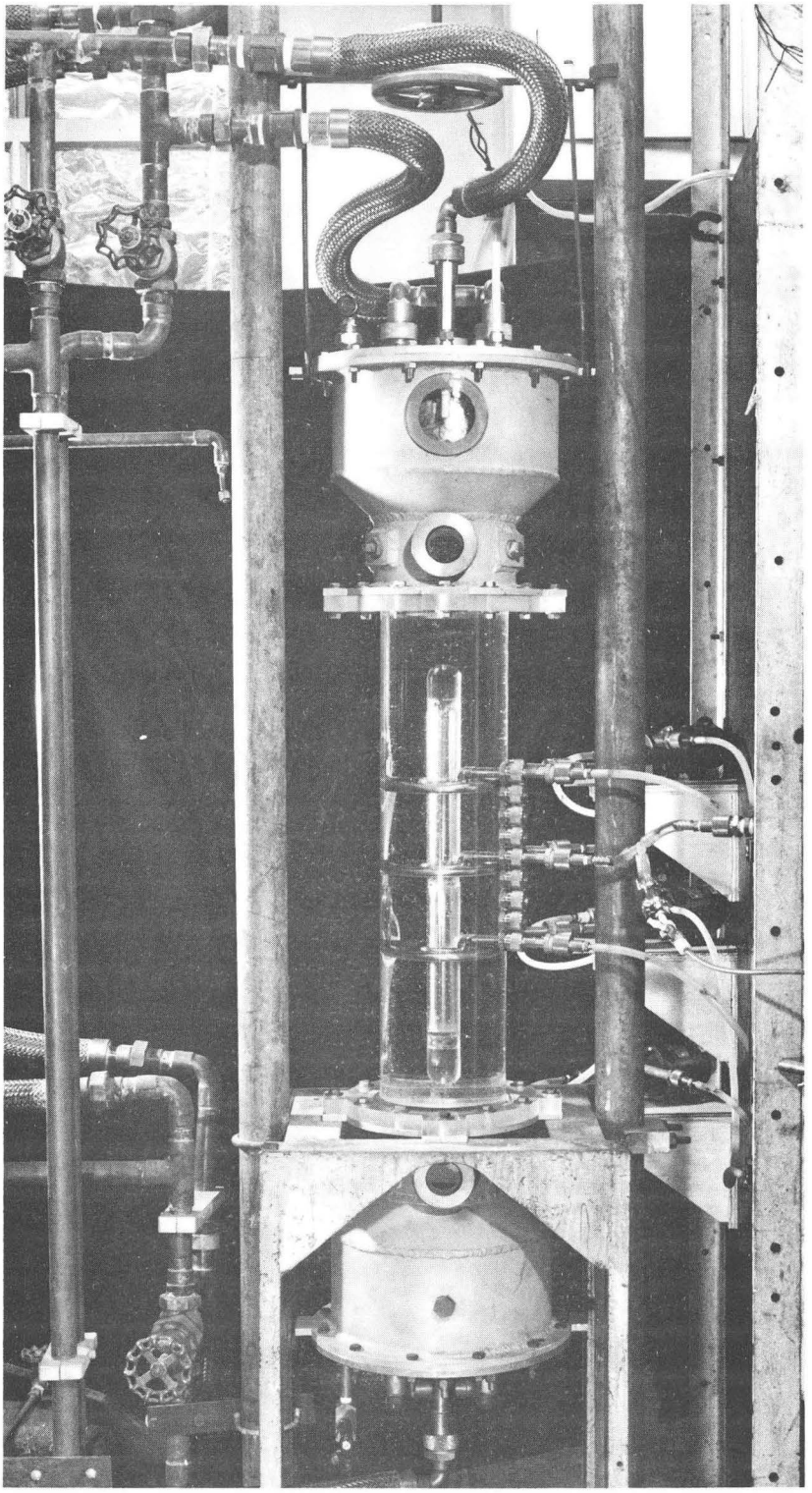

XBB 6812-7660

Fig. 19. Completed column assembly with central cylindrical wall.

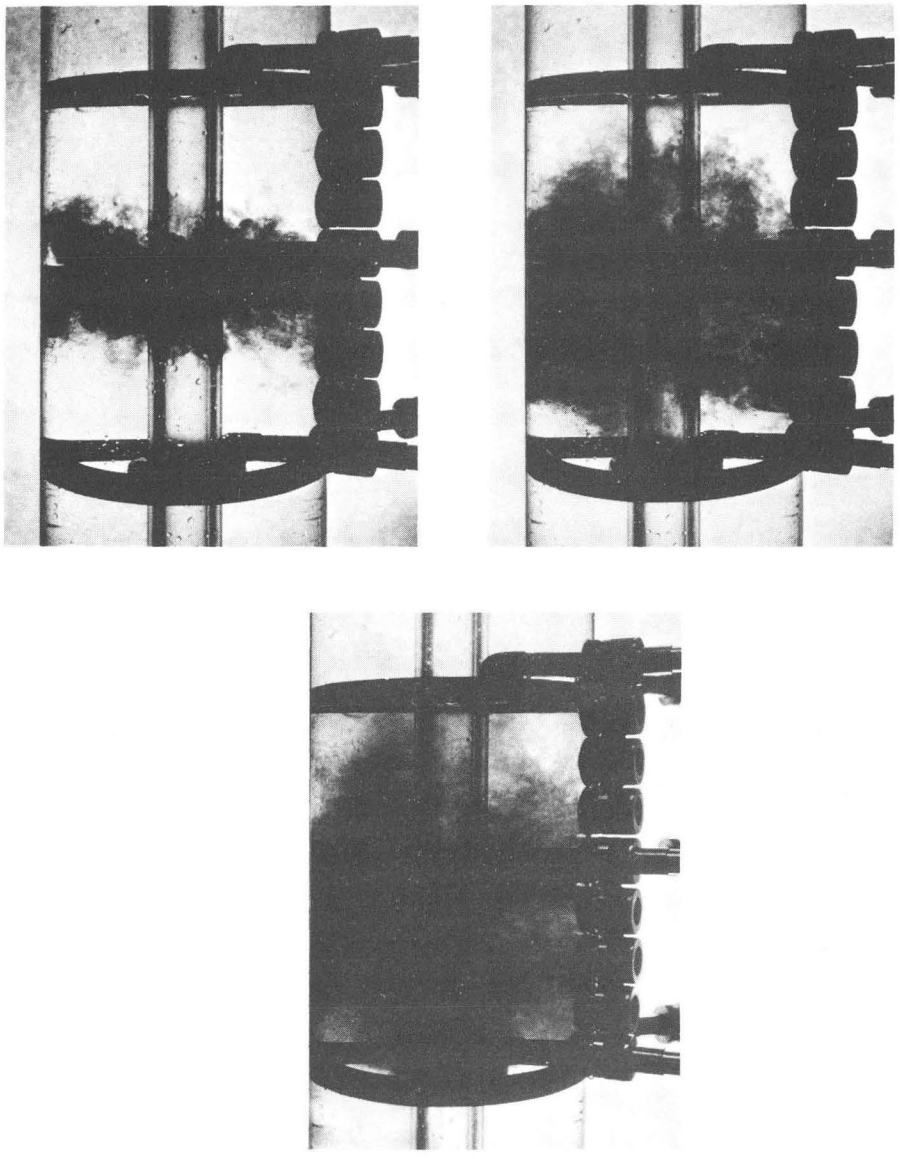

XBB 6812-7664

Fig. 20. Dye-mixing photographs ($h_c$ = 4 in., $F_c$ = 0.52 gal/min, and $F_r$ = 0.70 gal/min) following a one-second dye injection after (a) 1 sec, (b) 3 sec, and (c) 5 sec.

each stage and using a 6-in. column diameter, a 3-in. compartment height gave the best result, producing an effective vortex structure in each "stage" while avoiding overlap of vortices between adjacent compartments. Optimum stage spacing in a scaled-up version of the JMC will ultimately depend upon the relative importance of tower height and radial-pumping costs versus the desired degree of mass transfer and avoidance of axial dispersion.

d. Effect of Through Flow and Radial Flow Rate

Varying the overall flow rate ($F_c$) influenced directly the speed at which dye was swept out the lower end of the column. As $F_c$ was decreased, dye remained compartmentalized between ring stages for longer intervals of time, and vortex motion within each compartment was more easily discernable. Reducing the radial flow rate resulted in slower vortex motion, and hence less mixing. Varying $F_c$ or $F_r$ did not appear to alter appreciably the intrastage mixing patterns produced by the jetting rings.

e. Control of End Effects

With the central cylindrical wall in position, dye injection at stage 1 revealed slow, nonuniform vortex motion occurring more than one stage distance above this point. A similar observation was made below stage 3 immediately after injection at stages 2 or 3. Such end effects enhance longitudinal dispersion, and may be reduced by inserting a calming grid or wire-mesh screen approximately one-half to one stage height above the first stage and below the last stage in the column.

## B. Two-Phase Flow

### 1. Extraction Materials

Two-phase experimental trials were conducted with city water as the continuous phase and isododecane (IDD) as the dispersed phase. The IDD ("Chevron Isoparaffin 370"), a 350-400°F distillate fraction from sulfuric acid alkylate bottoms, was supplied through the courtesy of Chevron Research Co. The important physical properties of IDD for the present work are a density of 0.755 $g/cm^3$ (20°C), a viscosity of 2.4 cp (20°C), and an interfacial tension with water of 40.5 dynes/cm.

### 2. Intake-Ring Modifications

The purpose of the two-phase studies was to systematically test the effect of radial pumping rate and ring-port design, in order to determine the conditions which give the most intense mixing of the two liquids without producing a permanent emulsion.

For the same column designs described in Figure 18b and c, and with $F_c$ = 1.0 gal/min and $F_d$ = 0.3 to 1.0 gal/min, a milky emulsion was formed throughout the column at moderate radial flows (0.4 to 0.7 gal/min) without evidence of sufficient droplet breakup. The emulsion was attributed to the capture of rising organic droplets by the intake rings, the droplets becoming finely dispersed in the water phase as they passed through the radial centrifugal pumps. It was therefore necessary to develop a method that would retard this process and allow higher radial flow rates to be obtained.

A trial solution to the problem, which proved workable, was to soft-solder a 1/32-in.-thick curved brass disc or bonnet to the bottom of each intake ring. The bonnet extended to the level of the top of the ring, thus shielding the intake ports from the action of the jetting ports. The disc construction is shown in Figures 21 and 22 for both stage configurations. The insertion of such bonnets permits radial flows to be increased as high as 0.9 gal/min before the contents of the column becomes cloudy. This is illustrated in Figure 23, where a series of two-phase mixing photographs have been taken at the same longitudinal flow rates ($F_c$ = 0.75 gal/min and $F_d$ = 0.71 gal/min), but for varying radial flow rates. At 0.84 gal/min, a good dispersion is obtained without cloudiness, whereas at 0.98 gal/min, emulsion is being produced.

3. Jetting-Ring Modifications

A primary purpose of the jetting rings is to intercept the dispersed-phase droplets, entrain them into the local circulation patterns, intermix them by coalescence with other droplets if possible, and subdivide them by the local turbulence if they grow too large. In order to improve the interception of dispersed-phase droplets, the inner and outer jetting ring-port designs were modified by decreasing the hole diameter and increasing the number of ports. The total port cross-sectional area of the IRJ-8 ring was adopted, since this design showed strong jetting action with reasonably uniform flow. The four additional jetting rings designed on this basis are listed in Table 6 and are shown in Figures 24 and 25.


XBB 6812-7368

Fig. 21. Addition of brass bonnet to outer intake ring.


XBB 6812-7363

Fig. 22. Addition of brass bonnet to inner intake ring.

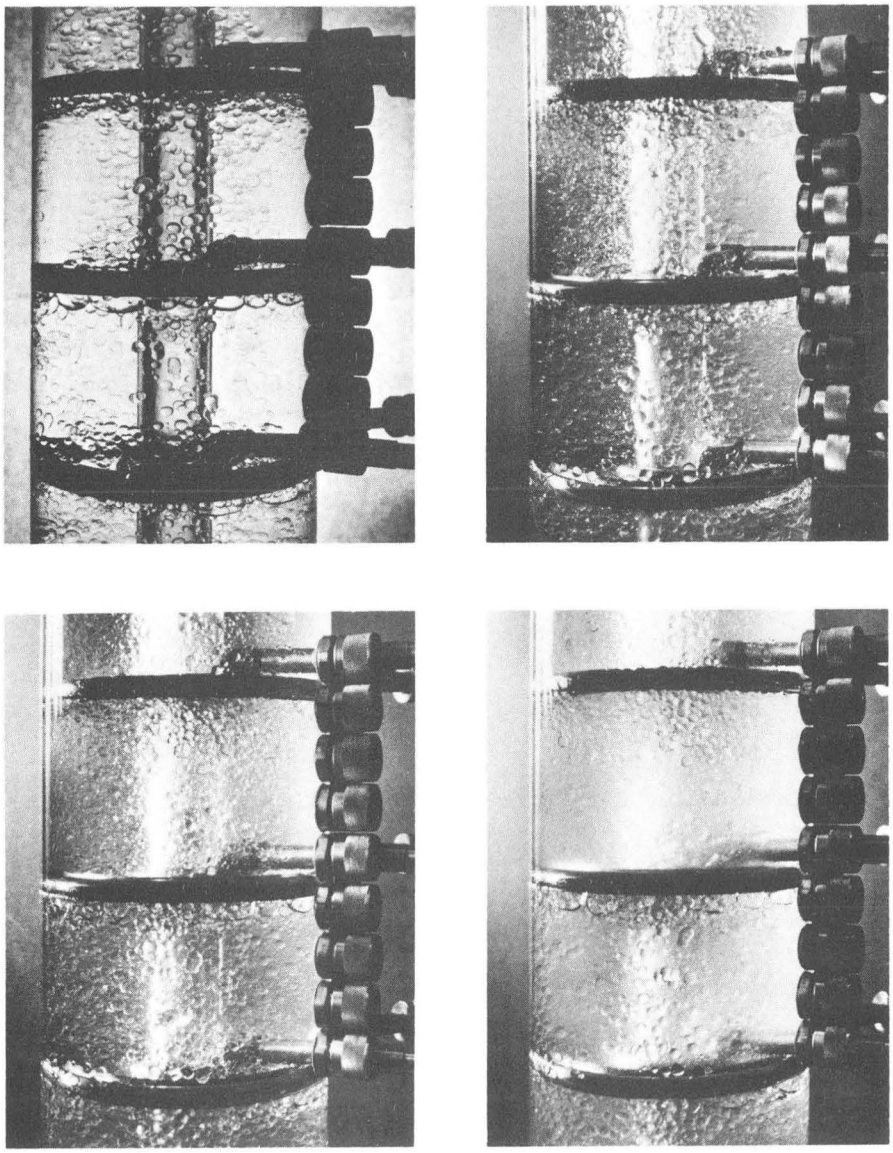

XBB 6812-7669

Fig. 23. Two-phase mixing in the jet-mixed column ($h_c$ = 4 in., $F_c$ = 0.75 gal/min, and $F_d$ = 0.71 gal/min): (a) $F_r$ = 0, (b) $F_r$ = 0.70 gal/min, (c) $F_r$ = 0.84 gal/min, and (d) $F_r$ = 0.98 gal/min.

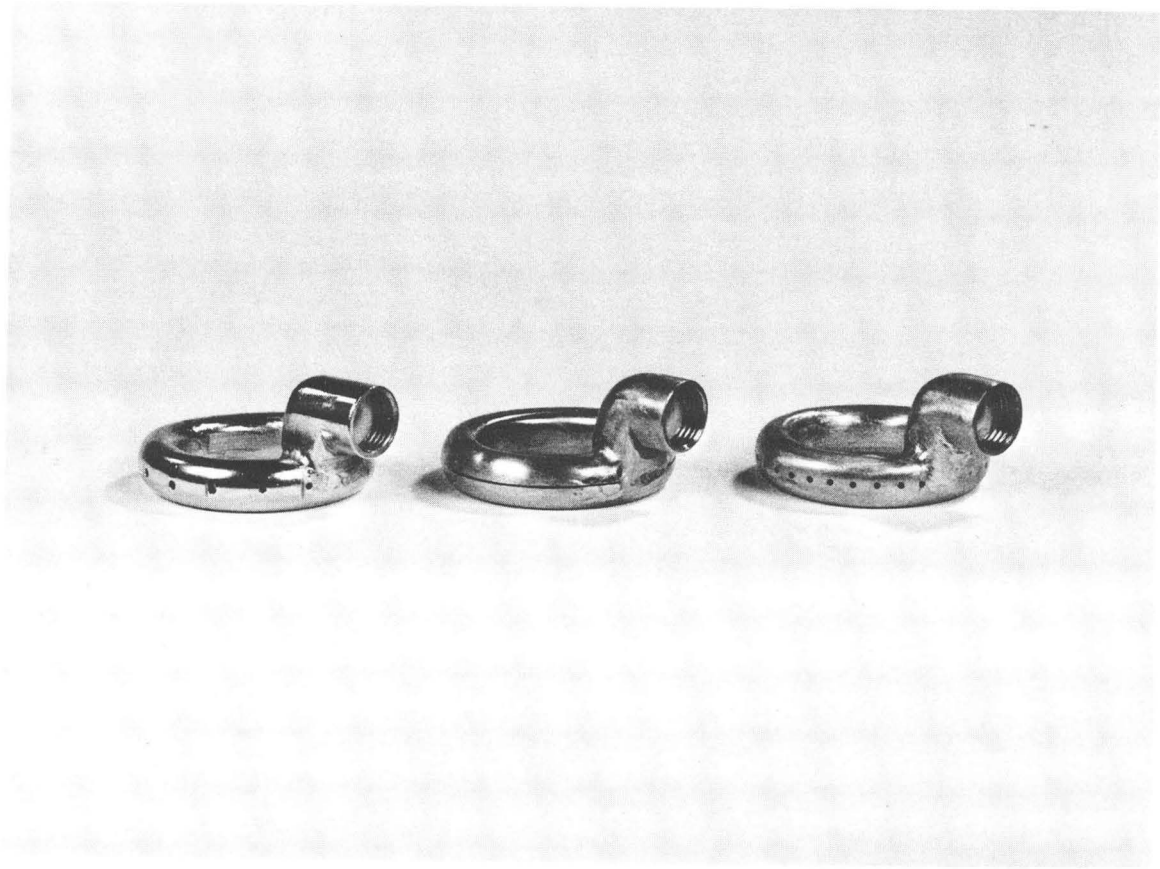

XBB 6812-7366

Fig. 24. Inner jetting-ring designs: (a) IRJ-15, (b) IRJ-slit, and (c) IRJ-29.

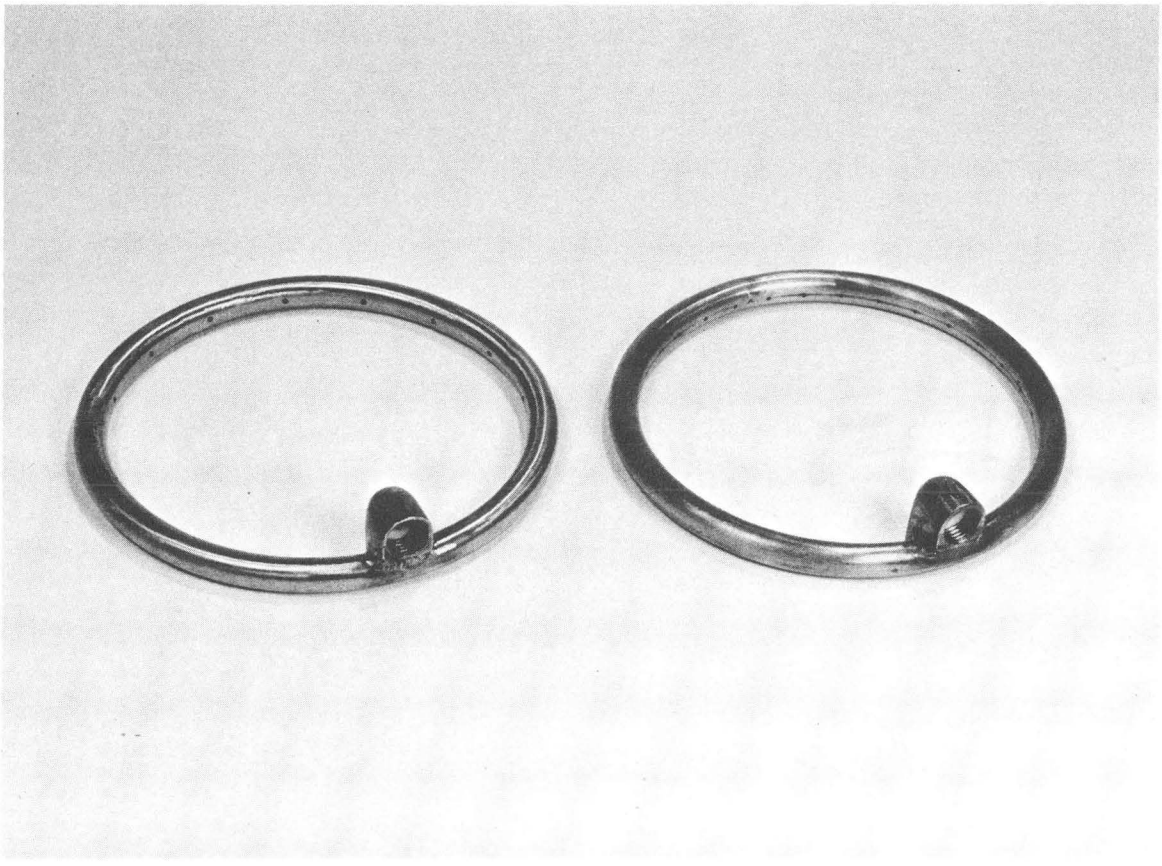

XBB 6812-7365

Fig. 25. Outer jetting-ring designs: (a) ORJ-16, and (b) ORJ-31.

Table 6

Summary of Jetting-Ring Designs

| Configuration | Number of Ports | Port Diameter (in) | Total Cross-Sectional Area of Ports ($in^2$) | $\frac{\sum A_p}{A_t}$ |
|---|---|---|---|---|
| IRJ | 8 | 3/32 | 0.055 (basis) | 0.92 |
| IRJ | 15 | 11 @ 1/64<br>4 @ 3/64 | 0.041 | 0.68 |
| IRJ | 29 | 3/64 | 0.050 | 0.83 |
| IRJ | continous slit | 1/64 thickness | 0.078 | 1.30 |
| ORJ | 16 | 1/16 | 0.049 | 0.82 |
| ORJ | 31 | 3/64 | 0.053 | 0.88 |

To examine visually the droplet-breakup effectiveness of each jetting ring, each inner jetting ring was connected to the ORW-31 (1/16-in.-dia. ports) bonneted ring, and each outer jetting ring was attached to the IRW-16 (3/32-in.-dia. ports) bonneted ring. The column was then operated at several flow ratios ($F_c/F_d$) and various radial flow rates (ranging from 0.3 to 1.0 gal/min). In addition, the flow distribution around each jetting ring was examined qualitatively by observing the flow into air through each port. From these tests, the best stage configuration was found to be IRJ(29)-ORW(31). This design was more effective in breaking up rising organic droplets than its counterpart, the ORJ(31)-IRW(16) configuration, for the same flow rates.

## C. Summary

The single-phase and two-phase flow experiments provided a basis for improved modifications in the initial design of the JMC. As a result of the manifold flow distribution along a jetting ring, the limiting-port-area criterion for the intake and jetting rings was revised to be:

$$\frac{\sum A_p}{A_t} \leq 2 \quad .$$

Hence the initial number of intake-ring ports was doubled.

Dye-injection studies showed that a central cylindrical wall placed through the inner rings was effective in eliminating longitudinal dispersion along the axis of the column. The dye tests also revealed that the IRJ-ORW configuration at each stage produced more efficient, localized mixing action than its counterpart, the ORJ-IRW configuration. For the former, two vortex rings of opposite sense were obtained within each compartment, whereas only one vortex ring was formed between stages of opposite configuration.

Brass bonnets added to the intake rings reduced the entrainment of discontinuous phase through the intake ring and line into the jetting pump, and permitted the maximum allowable radial flow rate to approach 1 gal/min before a milky emulsion formed. The interception of rising dispersed-phase droplets by effective jetting action in the column was enhanced by decreasing the diameter, and increasing the number, of jetting-ring ports.

The stage design:

IRJ-29 (3/64-in.-dia. ports)

ORW-31 (1/16-in.-dia. ports) ,

produced effective droplet breakup and intense mixing of the two phases at 0.84 gal/min, without forming a stable emulsion.

Excessive end-mixing was observed during the experiments. If the assembly of stages does not fill the column completely, as in the exploratory phase described here, a calming grid or wire-mesh screen should be inserted above the first stage and below the last stage in the column in future runs, in order to reduce end effects.

# V. SCHEDULE FOR FUTURE EXPERIMENTATION

## A. Apparatus Modifications

Appropriate modifications of the existing extraction apparatus should be made prior to further experimental work. First, to provide visual observation of the liquid-liquid interface for the case when water is the heavy dispersed phase, a 2.5-in.-dia. window should be provided in the lower column head, as has been done for the upper head (see Figure 11). Also, improvement in the liquid-level control system is needed to permit more rapid and accurate positioning of the interface at the desired constant level in either head. The present globe valve in the outlet water line (see Figure 16) requires continual adjustment. This situation can be improved by using the outlet globe valve for coarse interface adjustment, and the overflow arm, modified to slide easily upward or downward, for fine level control.

To evaluate convincingly the performance of the jet-mixed column will require a larger number of ring stages, and a series of organic-phase and aqueous-phase sampling probes along the column wall to indicate the internal concentration profiles. The size and spacing of the ring-stage holes, and the design of the column fittings at each hole, have been described in Section III-A. A discussion of sampling techniques will follow in Section V-B.

Nine pairs of inner and outer rings are available which are in, or convertible to, the optimum port layout. Since a 3-inch compartment

height has been found to produce satisfactorily localized continuous-phase mixing patterns, the present 24-inch column will accomodate eight stages and appears suitable for further study. If extensive study of 4-inch stage spacing seems desirable, a taller column should probably be constructed, and the existing column frame would take a 32-inch column section without major modifications. Wire screens of 1/4-in. to 3/8-in. mesh should be inserted one-half stage height above the first stage and below the last stage in the column in order to confine the circulation patterns created by the end stages.

## B. Extractor Performance Evaluation

The performance evaluation of the JMC should include the measurement of interfacial area, dispersed-phase holdup, flooding and emulsification limits, and column concentration profiles for several solvent-solute systems. The purpose of the following section, therefore, is to outline possible procedures and methods of approach for completing the above experimental schedule.

After such data become available, they should be compared to performance data of other mechanically aided column-type extractors, such as pulsed-plate, rotating-disc, and Oldshue-Rushton columns. The backflow or diffusion model for describing the combined effect of mass transfer and longitudinal dispersion may be used to correlate and interpret the results.

### 1. Measurement of Interfacial Area

Several methods are available to obtain good approximations

of interfacial area in the JMC. One involves determining the amount of light transmitted through the dispersion (48). A second, more tedious, technique requires two types of measurements. First, the average drop size of the dispersed phase is measured by taking photographs through the column wall (25,31,37,43). The total volume of dispersed phase present is then measured by any convenient means, as described in the next paragraph. From these two quantities, the number of drops, the surface area of the average drop, and finally the total interfacial area, may be calculated.

2. Holdup Measurements

With the column operating at steady state and the interface at a known level, the inlet and outlet flows and all radial jetting pumps should be stopped simultaneously. The increase in the interface level represents the volumetric holdup of dispersed phase. Correlation of the data will involve plots of dispersed-phase holdup versus discontinuous-phase flow rate, with radial jetting rate as the third variable parameter, at constant continuous-phase flow rates.

3. Flooding and Emulsification Limits

The maximum throughput obtainable, or flooding limits, of the JMC should be dtermined, including the effect of the jetting flow rates. Flooding develops, at any given flow rate of the continuous phase, when the dispersed-phase flow rate is maintained high enough so that the holdup increases markedly, the driving force for forward flow of dispersed

phase drops off, and the entering dispersed phase is discharged as an "underflow" with the effluent continuous phase.

Emulsification in the JMC at moderate jetting flow rates (1 gal/min) has been a problem in the present study. The occurrence of emulsification is a result of entrainment of discontinuous phase through the intake rings and into the jetting pumps, where the drops become finely dispersed in the continuous phase before being emitted through the jetting rings. An improved method to increase the emulsification limit would result in a decrease in dispersed-phase drop size, and an increase in the interfacial area for mass transfer.

4. Concentration-Profile Measurements

a. Extraction Systems

A minimum of two solvent-solute systems should be selected for the measurement of dispersed- and continuous-phase concentration gradients in the JMC. One suitable ternary system, which has been investigated by Moon and co-workers (40), is that of water—crotonic acid—isododecane. The distribution of crotonic acid between water and isododecane, as measured by Moon, is shown in Figure 26.

An alternate solvent, 2-ethyl hexanol, exhibiting a lower interfacial tension with water ($\sigma$ = 11.4 dynes/cm) than isododecane ($\sigma$ = 40.5 dynes/cm), has been found to be compatible with the present apparatus. A suitable solute for the water— 2-ethyl hexanol system remains to be chosen.

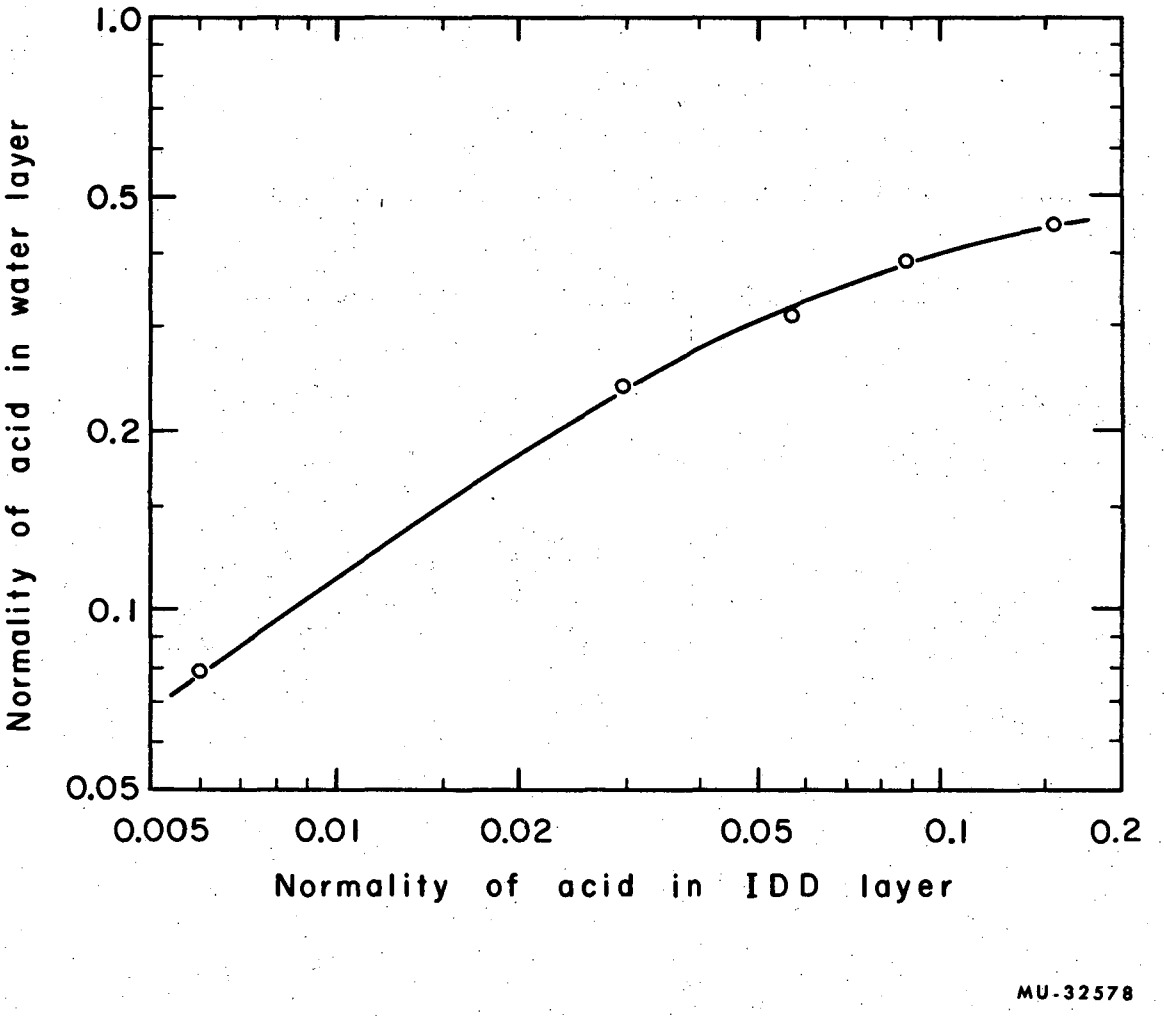


Fig. 26. Distribution of crotonic acid between water and isododecane.

b. Sampling Techniques

To obtain a concentration profile in the extractor, point concentrations of the solute in each phase need to be determined. The continuous phase can be sampled conveniently by drilling holes along the column wall to provide an entrance for hypodermic needles (25). The needles may be connected to individual collecting flasks by polyethylene or latex tubing, using pinch clamps to regulate the flow. Gier and Hougen (18) fitted sampling needles to 20-cc hypodermic syringes, each syringe resting upon a common support. By attaching two syringe stops to each sampling point, all continuous-phase samples were withdrawn simultaneously, at approximately the same rate and for the same total sample volume.

Discontinuous-phase sampling can be achieved by several means. Moon and co-workers (40) used a probe consisting of a 0.75-in.-dia. bakelite sphere into which a 0.5-in. hole was drilled. A sampling tube extended through the wall of the sphere, and the entire probe was pointed in the direction that would trap the moving droplets. A thin disk of teflon felt was cemented into the mouth of the cylindrical cavity in the sphere to give selective flow of the organic phase. As an alternate method, hypodermic needles may be packed with a granular material preferentially wet by the dispersed phase (25). For any design, the sampling probe should be made as small as possible to minimize flow obstruction.

Continuous- and discontinuous-phase samples may either be taken at the same level in the column, or staggered in position. For the former, the point concentrations obtained should not be considered as those of passing streams, since no direction flow is clearly indicated. It would be interesting to obtain several samples of each phase at the same column cross-section, and in the same stage compartment, to investigate jet-mixing efficiency.

Samples should not be taken until the interface has been held constant with the column operating at steady state. Common practice is to allow sufficient feed to be introduced to change the contents of the column three or four times. The sampling rates of each phase should be less than 1% of the total flow rate, as Geankoplis (17) found this rate to have little effect on column operation.

c. Method of Analysis

For the water—crotonic acid— isododecane system, the amount of acid in each sample can be determined by titration with 0.1 N and 0.01 N standard sodium hydroxide solutions, with 0.05% phenolphthalein as indicator.

The continuous-phase samples will probably contain negligible amounts of dispersed phase. However, discontinuous-phase samples with continuous-phase contamination are likely to occur. These samples must be corrected, as mass transfer will be taking place during sampling and prior to analysis. One procedure is to deliberately allow the two phases

to reach equilibrium by vigorous shaking of the samples. A material balance for this process gives:

$$V_w C_{w_o} + V_s C_{s_o} = V_w C_{w_e} + V_s C_{s_e} = V_w C_{w_e} + V_s K C_{w_e} \quad , \qquad (22)$$

where

$V_w$, $V_s$ = volume of aqueous and organic phases, respectively, in each sample, cc,

$C_{w_o}$, $C_{s_o}$ = concentration of solute in aqueous and organic phases, respectively, just prior to sampling, g-moles/cc,

$C_{w_e}$, $C_{s_e}$ = equilibrium concentration of solute in aqueous and organic phases, respectively, g-moles/cc, and

$K$ = equilibrium distribution constant of solute between organic and aqueous phases, $C_{s_e}/C_{w_e}$.

Introducing the volumetric sample ratio, $\phi = V_s/V_w$, and rearranging Equation (22) yields:

$$C_{w_o} = C_{w_e} (1 + K\phi) - C_{s_o}\phi \qquad (23)$$

and

$$C_{s_o} = C_{s_e} (1 + 1/K\phi) - C_{w_o}/\phi \quad . \qquad (24)$$

At least one pair of two-phase samples with unequal values of $\phi$ is necessary to simultaneously solve these equations.

Among many extraction studies in the literature, almost none include interior concentration measurements. The recently developed understanding of axial dispersion has made it evident that interpretation of column performance is inaccurate if not impossible in the absence of such internal measurements.

## NOMENCLATURE

$a$ = specific interfacial area of mixed phases, $cm^2/cc$

$A_p$ = area of a port in a tubular jetting or intake ring, $in^2$

$A_t$ = inner cross-sectional area of a tubular ring, $in^2$

$b$ = intercept value for partition equilibrium, in the relation $c_x^* = b + mc_y$, gram-moles/cc

$B$ = dimensionless height, L/d

$c_i$ = concentration of solute in ith phase, gram-moles/cc

$C_i$ = $c_i/c_x^0$ (dimensionless), with $c_x^0$ the feed-stream concentration

$C_{w_e}, C_{s_e}$ = equilibrium concentration of solute in aqueous and organic phases, respectively, gram-moles/cc

$C_{w_o}, C_{s_o}$ = concentration of solute in aqueous and organic phases, respectively, just prior to sampling, gram-moles/cc

$d$ = characteristic local length of equipment, cm

$\overline{E}_i$ = superficial longitudinal dispersion coefficient in the ith phase, $cm^2/sec$

$\overline{F}_i$ = mean volumetric flow rate of main (through) flow for ith phase, $cc/cm^2$-sec

$\overline{F}_i$ = volumetric rate of interstage mixing for ith phase, $cc/cm^2$-sec

$F$ = sum of the volumetric rates of interstage mixing for phases X and Y, $cc/cm^2$-sec

$F_c$ = volumetric flow rate of continuous phase, gal/min

$F_d$ = volumetric flow rate of discontinuous phase, gal/min

$F_r$ = volumetric jetting flow rate, gal/min

$h_c$ = compartment height in the jet-mixed column, in

$k_{oi}$ = over-all coefficient of mass transfer based on ith phase, cm/sec

$K$ = equilibrium distribution constant of solute between organic and aqueous phases, $C_{s_e}/C_{w_e}$, dimensionless

$l_i$ = effective mixing length, $\overline{E}_i/\overline{F}_i$, cm

$L$ = height of column, cm

$L_o$ = stage height, cm

$m$ = equilibrium partition coefficient, in the relation $c_x^* = b + mc_y$, dimensionless

$n_p$ = total number of stages, dimensionless

$N_{oi}$ = number of over-all transfer units in column based on ith phase, $k_{ox}aL/\overline{F}_i$, dimensionless

$P_i$ = local Peclet number for ith phase, $d/l_i$, dimensionless

$P_iB$ = column Peclet number for ith phase, $L\overline{F}_i/\overline{E}_i$, dimensionless

$Q$ = $b/c_x^0$, dimensionless

$V_w, V_s$ = volume of aqueous and organic phases, respectively, in each sample, cc

$X$ = generalized solute concentration in X-phase, $\left[c_x - (Q + mc_y^1)\right] / \left[1 - (Q + mc_y^1)\right]$, dimensionless

$Y$ = generalized solute concentration in Y-phase, $m(C_y - C_y^1) \Big/ \left[1 - (Q + mC_y^1)\right]$, dimensionless

$z$ = length within column, measured from X-phase inlet in direction of flow, cm

$Z$ = fractional length in column, z/L, dimensionless

$\Lambda$ = extraction factor, $m\overline{F}_x/\overline{F}_y$, dimensionless

$\sigma$ = interfacial tension, dynes/cm

$\phi$ = volumetric sample ratio, $V_s/V_w$, dimensionless

Subscripts

F = feed-end value

i = designates phase concerned, either X or Y

j = stage number

L = outlet-end value

o = over-all

x,y = X or Y phase

0 = feed-inlet end, inside column

1 = feed-outlet end, inside column

Superscripts

* = equilibrium value

0 = feed-inlet end, outside column

1 = feed-outlet end, outside column

ACKNOWLEDGMENT

The research was performed under the joint auspices of the U. S. Atomic Energy Commission and the University of California College of Chemistry. The first-named author acknowledges with thanks a National Defense Education Act Title IV Fellowship.

The gift of the isododecane supply (Chevron Isoparaffin 370) from Chevron Research Company is gratefully acknowledged. The authors also thank G. G. Young and Carl Baugh for their work in the mechanical construction of the column and accessory fittings.

Figures 3 through 6 are adapted from the papers by T. Miyauchi; Figures 11, 13, and 16 are modified from those initially given in reports by G. Jacques; and Figure 26 is taken from a report by J. S. Moon.

## REFERENCES


1. A. Acrivos, B. D. Babcock, and R. L. Pigford, Chem. Eng. Sci., 10, 112 (1959).
2. R. B. Akell, Chem. Eng. Prog., 62, (9), 50 (1966).
3. R. E. Bibaud and R. E. Treybal, A.I.Ch.E. Journal, 12, 472 (1966).
4. A. H. Brown and C. Hanson, Trans. Faraday Soc., 61, 1754 (1965).
5. L. L. Burger and W. H. Swift, U. S. Atomic Energy Comm., Hanford Works, Report HW-29010 (1953).
6. E. J. Cairns and J. M. Prausnitz, Chem. Eng. Sci., 12, 20 (1960).
7. J. J. Carberry and R. H. Bretton, A.I.Ch.E. Journal, 4, 367 (1958).
8. W. A. Chantry, R. L. Von Berg, and H. F. Wiegandt, Ind. Eng. Chem. 47, 1155 (1955).
9. C. M. Christensen, Liquid-Liquid Extraction Efficiencies of a Pulsed Packed Column and a Pulsed Sieve-Plate Column of Four-Inch Diameter (Ph.D. Thesis), Cornell University, 1961.
10. M. W. Davis, Jr., T. E. Hicks, and T. Vermeulen, Chem. Eng. Prog., 50, 188 (1954).
11. E. A. Ebach and R. R. White, A.I.Ch.E. Journal, 4, 161 (1958).
12. W. Eguchi and S. Nagata, Chem. Eng. (Japan), 22, 218 (1958).
13. W. Eguchi and S. Nagata, ibid., 23, 146 (1959).
14. H. Eisenlohr and A. Scharlan, Pharm. Ind., 17, 207 (1955).
15. G. Feick and H. M. Anderson, Ind. Eng. Chem., 44, 405 (1952).
16. C. J. Geankoplis and A. N. Hixson, ibid., 42, 1141 (1950).
17. C. J. Geankoplis, P. J. Wells, and E. L. Hawk, ibid., 43, 1848 (1951).

18. T. E. Gier and J. O. Hougen, ibid., 45, 1362 (1953).

19. E. B. Gutoff, A.I.Ch.E. Journal, 11, 712 (1965).

20. C. Hanson, Chem. Eng., 75, (18), 176 (1968).

21. C. Hanson, ibid., 75, (19), 135 (1968).

22. S. Hartland and J. C. Mecklenburgh, Chem. Eng. Sci., 21, 1209 (1966).

23. D. E. Hazebeck and C. J. Geankoplis, Ind. Eng. Chem. Fund., 2, 310 (1963).

24. A. N. Hennico, G. L. Jacques, and T. Vermeulen, U. S. Atomic Energy Comm., Report UCRL-10696 (1963).

25. J. R. Honekamp and L. E. Burkhart, Ind. Eng. Chem. Proc. Des. Dev., 1, 177 (1962).

26. G. L. Jacques, J. E. Cotter, and T. Vermeulen, U. S. Atomic Energy Comm., Report UCRL-8658 (1959).

27. G. L. Jacques and T. Vermeulen, U. S. Atomic Energy Comm., Report UCRL-8029 (1957).

28. H. F. Johnson and H. Bliss, Trans. Am. Inst. Chem. Engrs., 42, 331 (1946).

29. R. M. Krieger and C. J. Geankoplis, Ind. Eng. Chem., 45, 2156 (1953).

30. N. N. Li and E. N. Ziegler, ibid., 59, (3), 30 (1967).

31. R. Letan and E. Kehat, A.I.Ch.E. Journal, 13, 443 (1967).

32. B. W. Mar and A. L. Babb, Ind. Eng. Chem., 51, 1011 (1959).

33. A. K. McMullen, T. Miyauchi, and T. Vermeulen, U. S. Atomic Energy Comm., Report Supplement UCRL-3911 (1958).

34. S. F. Miller and C. J. King, A.I.Ch.E. Journal, 12, 767 (1966).

35. T. Miyauchi, U. S. Atomic Energy Comm., Report UCRL-3911 (1957).

36. T. Miyauchi, H. Mitsutake, and I. Harase, A.I.Ch.E. Journal, 12, 508 (1966).

37. T. Miyauchi and H. Ohya, ibid., 11, 395 (1965).

38. T. Miyauchi and T. Vermeulen, Ind. Eng. Chem. Fund., 2, 113 (1963).

39. T. Miyauchi and T. Vermeulen, ibid., 2, 304 (1963).

40. J. S. Moon, A. N. Hennico, and T. Vermeulen, U. S. Atomic Energy Comm., Report UCRL-10928 (1963).

41. V. S. Morello and N. Poffenberger, Ind. Eng. Chem., 42, 1021 (1950).

42. J. Y. Oldshue and J. H. Rushton, Chem. Eng. Prog., 48, 297 (1952).

43. R. B. Olney, A.I.Ch.E. Journal, 10, 827 (1964).

44. W. J. Podbielniak, Chem. Eng. Prog., 49, 252 (1953).

45. G. H. Reman, ibid., 62, (9), 56 (1966).

46. G. H. Reman and R. B. Olney, ibid., 51, 141 (1955).

47. V. Rod, Brit. Chem. Eng., 11, 483 (1966).

48. W. A. Roger, U. S. Atomic Energy Comm., Report ANL-5575 (1956).

49. E. G. Scheibel, Chem. Eng. Prog., 44, 681 (1948).

50. E. G. Scheibel, A.I.Ch.E. Journal, 2, 74 (1956).

51. E. G. Scheibel and A. E. Karr, Ind. Eng. Chem., 42, 1048 (1950).

52. G. A. Sehmel and A. L. Babb, Ind. Eng. Chem. Proc. Des. Dev., 3, 210 (1964).

53. T. Shirotsuka, N. Honda, and T. Yasumo, Chem. Eng. (Japan), 21, 645 (1957).

54. C. A. Sleicher, A.I.Ch.E. Journal, 5, 145 (1959).

55. C. A. Sleicher, ibid., 6, 529 (1960).

56. L. D. Smoot and A. L. Babb, Ind. Eng. Chem. Fund., 1, 93 (1962).

57. L. D. Smoot, B. W. Mar, and A. L. Babb, Ind. Eng. Chem., 51, 1005 (1959).

58. E. P. Stainthorp and N. Sudall, Trans. Inst. Chem. Engrs., 42, T198 (1964).

59. S. Stemerding, E. C. Lumb, and J. Lips, Chem.-Ing.-Tech., 35, 844 (1963).

60. C. P. Strand, R. B. Olney, and G. H. Ackerman, A.I.Ch.E. Journal, 8, 252 (1962).

61. J. D. Thornton, Chem. Eng. Prog. Symp. Series, 50, No. 13, 39 (1954).

62. J. D. Thornton, ibid., 50, No. 13, 179 (1954).

63. T. Vermeulen, J. S. Moon, A. Hennico, and T. Miyauchi, Chem. Eng. Prog., 62, 95 (1966).

64. H. G. Vogt and C. J. Geankoplis, Ind. Eng. Chem., 46, 1763 (1954).

65. R. L. Von Berg and H. F. Wiegandt, Chem. Eng., 59, 189 (1952).

66. K. R. Westerterp and P. Landsman, Chem. Eng. Sci., 17, 363 (1962).

67. K. R. Westerterp and W. H. Meyberg, ibid., 17, 373 (1962).

*TECHNICAL INFORMATION DIVISION*
*LAWRENCE RADIATION LABORATORY*
*UNIVERSITY OF CALIFORNIA*
*BERKELEY, CALIFORNIA 94720*